

DOE STTR Phase I Final Scientific/Technical Report

Fabrication of Chemically Doped, High Upper Critical Field Magnesium Diboride Superconducting Wires

Summary

Controlled chemical doping of magnesium diboride (MgB_2) has been shown to substantially improve its superconducting properties to the levels required for high field magnets, but the doping is difficult to accomplish through the usual route of solid state reaction and diffusion. Further, superconducting cables of MgB_2 are difficult to fabricate because of the friable nature of the material.

In this Phase I STTR project, doped and undoped boron fibers were made by chemical vapor deposition (CVD). Several >100m long batches of doped and undoped fiber were made by CVD codeposition of boron plus dopants. Bundles of these fibers infiltrated with liquid magnesium and subsequently converted to MgB_2 to form Mg- MgB_2 metal matrix composites. In a parallel path, doped boron nano-sized powder was produced by a plasma synthesis technique, reacted with magnesium to produce doped MgB_2 superconducting ceramic bodies. The doped powder was also fabricated into superconducting wires several meters long.

The doped boron fibers and powders made in this program were fabricated into fiber-metal composites and powder-metal composites by a liquid metal infiltration technique. The kinetics of the reaction between boron fiber and magnesium metal was investigated in fiber-metal composites. It was found that the presence of dopants had significantly slowed the reaction between magnesium and boron. The superconducting properties were measured for MgB_2 fibers and MgB_2 powders made by liquid metal infiltration. Properties of MgB_2 products (J_c , H_{c2}) from Phase I are among the highest reported to date for MgB_2 bulk superconductors.

Chemically doped MgB_2 superconducting magnets can perform at least as well as NbTi and NbSn3 in high magnetic fields and still offer an improvement over the latter two in terms of operating temperature. These characteristics make doped MgB_2 an effective material for high magnetic field applications, such as magnetic confined fusion, and medical MRI devices. Developing fusion as an energy source will dramatically reduce energy costs, global warming, and radioactive waste. Cheaper and more efficient medical MRI devices could lower examination costs, find potential health problems earlier, and thus also benefit society as a whole. Other potential commercial applications for this material are devices for the generation and storage of electrical power, thus lowering the cost of delivered electricity.

Fabrication of Chemically Doped, High Upper Critical Field Magnesium Diboride Superconducting Wires

TABLE OF CONTENTS

	<u>Page No.</u>
1.0 Significance, Background Information, and Technical Approach.....	7
1.1 Identification and Significance of the Problem or Opportunity, and Technical Approach.....	7
1.1.1 Introduction.....	7
1.1.2 Property Improvements in MgB ₂ by Dopant Additions.....	7
1.1.3 Processing Approaches.....	8
1.1.4 Background.....	9
1.1.5 Initial Experiments.....	11
1.1.6 Liquid Metal Reaction.....	14
1.1.7 Boron Powder Synthesis.....	16
1.1.8 Powder-in-tube Wire Processing.....	19
1.2 Anticipated Public Benefits.....	22
1.3 Degree to Which Phase I has Demonstrated Technical Feasibility.....	27
1.3.1 Fabrication of Doped Boron Fibers by CVD.....	27
1.3.2 Liquid Metal Infiltration of Boron Fibers.....	27
1.3.3 Kinetics of the Reaction Between Boron Fibers and Mg Metal.....	28
1.3.3.1 Undoped Boron Fibers.....	28
1.3.3.2 Doped Boron Fibers.....	32
1.3.4 Initial Studies to Identify the Reaction Mechanism.....	34
1.3.4.1 Characterization Equipment.....	34
1.3.4.2 Results.....	34
1.3.5 Superconducting Properties of MgB ₂ Made by Liquid Metal Infiltration.....	38
1.3.6 Plasma Synthesis of Doped Boron Nano-sized Powder.....	38
1.3.7 Liquid Metal Infiltration of Plasma Synthesized Doped Boron Nano-sized Powder.....	38
1.3.8 Fabrication of Wire by PIT Using Doped Boron Nano-sized Powder....	39
2.0 Suggested Further Work.....	42
2.1 Technical Objectives of Further Work.....	42

2.2	Suggested Commercialization Plan	44
2.2.1	Company Information.....	44
2.2.2	Market	45
2.2.3	Intellectual Property.....	51
3.0	References.....	52

LIST OF FIGURES

<u>Figure No.</u>	<u>Page No.</u>
1. Process diagram showing CVD synthesis of boron fiber [1] and conversion to MgB ₂ by reaction with magnesium vapor [3-7, 9] or molten Mg [8].....	8
2. Process diagram for MgB ₂ wire from plasma synthesized doped boron powder	9
3. Cover art: MgB ₂ made from Specialty Materials boron fiber shown on the covers of <i>Physics Today</i> (March, 2003) [10], <i>Physics World</i> (January, 2002), and in <i>Scientific American</i> (April, 2005)	10
4. Single crystal of MgB ₂ doped with TiB (dark inclusions) [6]	12
5. Plot of values of J _c versus magnetic field at 5K for Ti-doped MgB ₂ reacted at 950°C [6]	12
6. Critical current density vs. magnetic field at 20K for Ti-doped wire samples made from CVD boron fibers [7].....	13
7. MgB ₂ made from doped boron fiber	13
8. Optical micrograph of fully reacted 200µm MgB ₂ fiber in Mg matrix under cross-polarized light (original B fiber was 140µm in diameter).....	14
9. Magnetic moment versus temperature under zero field conditions for single MgB ₂ fiber extracted from the reacted composite.....	15
10. Optical micrograph of partially reacted MgB ₂ fiber in Mg matrix	16
11. Chamber used for RF plasma synthesis of pure and doped boron nanopowders	17
12. Sub-micron boron powder produced via a plasma synthesis technique by the collaboration of SMI and SUNY at Stony Brook	17
13. X-ray diffraction patterns (Cu K _α radiation) of MgB ₂ made from pure and doped plasma synthesized boron powder	17
14. Properties of MgB ₂ made from plasma synthesized doped boron powder	17
15. Critical current density vs field at 5 K (solid points) and 20K (open points) of carbon-doped MgB ₂ made from plasma synthesized carbon-doped boron powder	18
16. Upper critical magnetic field data [8] for samples prepared from C-doped boron powder showing H _{c2} (T=0) ~ 37 tesla.....	18

17.	Optical micrograph of a polished cross section of a superconducting wire formed by the powder-in-tube (PIT) method.....	20
18.	Comparison of 5K critical current density data (J_c) for wires reacted at different temperatures for 30 min [8].....	20
19.	Experimental setup showing the reaction chamber used for in situ x-ray diffraction measurements.....	29
20.	Plot tracking the reaction between Mg and undoped boron fibers at various temperatures.....	29
21.	Reaction rate plots $Mg + B_{\text{fiber}} \rightarrow MgB_2$	30
22.	Polarized optical micrographs of Mg/MgB ₂ composites showing cross sections of fibers that have reacted to MgB ₂ at progressive stages of completion	30
23.	Fiber-Mg composite in which the boron fiber partially reacted with Mg.....	31
24.	Energy dispersive x-ray spectral (EDS) image of partially reacted fiber cross section showing unreacted boron, MgB ₇ , MgB ₄ , and MgB ₂	31
25.	Mg-B phase diagram.....	32
26.	Ti-doped boron fiber 38% reacted with Mg (36 hr, 1000°C)	33
27.	Doped boron fibers reacted with Mg in a metal matrix composite produced by liquid metal infiltration	33
28.	Surface morphology of boron fibers at the following carbon dopant levels in atomic percent: a) 0% b) 1.4% c) 2% and d) 3%.....	35
29.	X-ray diffraction patterns of undoped and carbon-doped B fibers	35
30.	Bright-field TEM image with Selected Area Diffraction (SAD).....	36
31.	TEM of interface between carbon doped boron fiber and Mg metal in a fiber-metal composite made by liquid Mg infiltration	37
32.	Critical current densities of 0.5% C-doped fibers.....	38
33.	Optical micrograph of a polished section showing synthesized boron powder infiltrated with liquid magnesium.....	39
34.	X-ray diffraction patterns of boron nanopowders infiltrated with liquid Mg and	

then further reacted for 1 hr at 1000°C	40
35. Superconducting properties of composites made by the infiltration of doped and undoped boron nanopowder.....	40
36. Comparison of J_C data for PIT wires made from plasma synthesized doped boron nanopowder.....	41

LIST OF TABLES

<u>Table No.</u>	<u>Page No.</u>
1. Comparison of the Cost/Performance (C/P) of several LTS and HTS wire technologies	23
2. Cost of ownership of wire specification for several conducting materials in temperature and magnetic field relevant to transformer applications.....	24
3. Cost of Various Conducting Materials (\$ per kA-m)	25
4. World Markets for Superconductors (\$M)	46
5. World Markets for Superconductors (\$M)	47
6. Estimated Milestones for Various Superconductor Applications.....	48

Fabrication of Chemically Doped, High Upper Critical Field Magnesium Diboride Superconducting Wires

1.0 Significance, Background Information, and Technical Approach

1.1 Identification and Significance of the Problem or Opportunity, and Technical Approach

1.1.1 Introduction

The discovery of superconductivity in magnesium diboride (MgB_2) at temperatures near 40K [1] has provided a technical opportunity to achieve high performance superconductors with low fabrication costs and lowered operating costs. In the four years since this 2001 discovery, significant progress has been made in the relatively new field of MgB_2 superconductors. Much of the initial work was focused on raising the superconducting transition temperature (T_c) by modifying the composition and crystal structure of pure MgB_2 via chemical substitution and/or the addition of dopant impurities. To date, all such modifications have resulted in a decrease in T_c . However, progress has been made in improving other very important superconducting properties, namely the critical current density (J_c) and the upper critical magnetic field (H_{c2}). This has kept MgB_2 in the forefront of importance in the field of superconductivity. Although at present MgB_2 -based devices cannot operate at temperatures at or near liquid nitrogen (77K) as do the Generation II YBCO coated conductors, there remain important reasons, both technological and economic, for the continuation of research and development efforts to produce practical MgB_2 devices. One significant reason is that the 40K superconducting transition of MgB_2 remains significantly higher than the classical low temperature superconductors (LTS) such as Nb_3Sn (18K) and NbTi (11K), which must be operated using liquid helium. MgB_2 devices are open to a practical operation temperature in the 20-25K range, which can be achieved by using closed cycle mechanical refrigeration or by using higher boiling cryogenics such as liquid neon or liquid hydrogen. Furthermore, if progress continues in the improvement of J_c and H_{c2} in MgB_2 superconductors, they could also surpass and supplant the LTS materials in devices operated at liquid helium temperature. Another significant reason to vigorously pursue R&D efforts in MgB_2 is an economic one. Although much progress has been made recently with Generation II YBCO high temperature superconductors [2,3] these materials may still be several years away from economic viability. In addition, the two-dimensional nature of the YBCO crystal structure results in anisotropic superconducting properties, so that these materials are not amenable to many standard and economic wire forming processes. A major focus of MgB_2 research and development is the fabrication of a low-cost conductor.

1.1.2 Property Improvements in MgB_2 by Dopant Additions

Joint experiments at Specialty Materials Inc. (SMI) and Iowa State University [4-7] have demonstrated that doping a boron fiber starting material by co-deposition of the dopant and boron through chemical vapor deposition (CVD) yields greatly improved superconductor properties when the material is converted to magnesium diboride. Significant increases relative to undoped MgB_2 have been demonstrated in both the critical current, ($J_c = 5 \times 10^6 \text{ A cm}^{-2}$ in titanium-doped MgB_2) and the upper critical magnetic field ($H_{c2}(0) \sim 35\text{T}$ in carbon-doped MgB_2). Recent results [8] on MgB_2 made from plasma synthesized nano-sized carbon-doped boron exhibited $J_c > 10^5 \text{ A cm}^{-2}$ at 5 tesla and $H_{c2}(0) \sim 37\text{T}$, the highest upper critical field

reported to date for bulk MgB_2 . Other workers have shown that additions of SiC [9], YB_4 [10], TiB_2 [11], and Mg_2Si [12] may be used to increase J_c .

1.1.3 Processing Approaches

J.D. DeFouw and D.C. Dunand [13] of Northwestern University have demonstrated the casting of boron fibers in a magnesium matrix with subsequent conversion to MgB_2 fibers. Hence, the potential exists for a process, based largely on existing commercial technology (boron filaments are manufactured by Specialty Materials at typical lengths > 10 km) to produce continuous, optimally doped magnesium diboride superconducting wire (Figure 1).

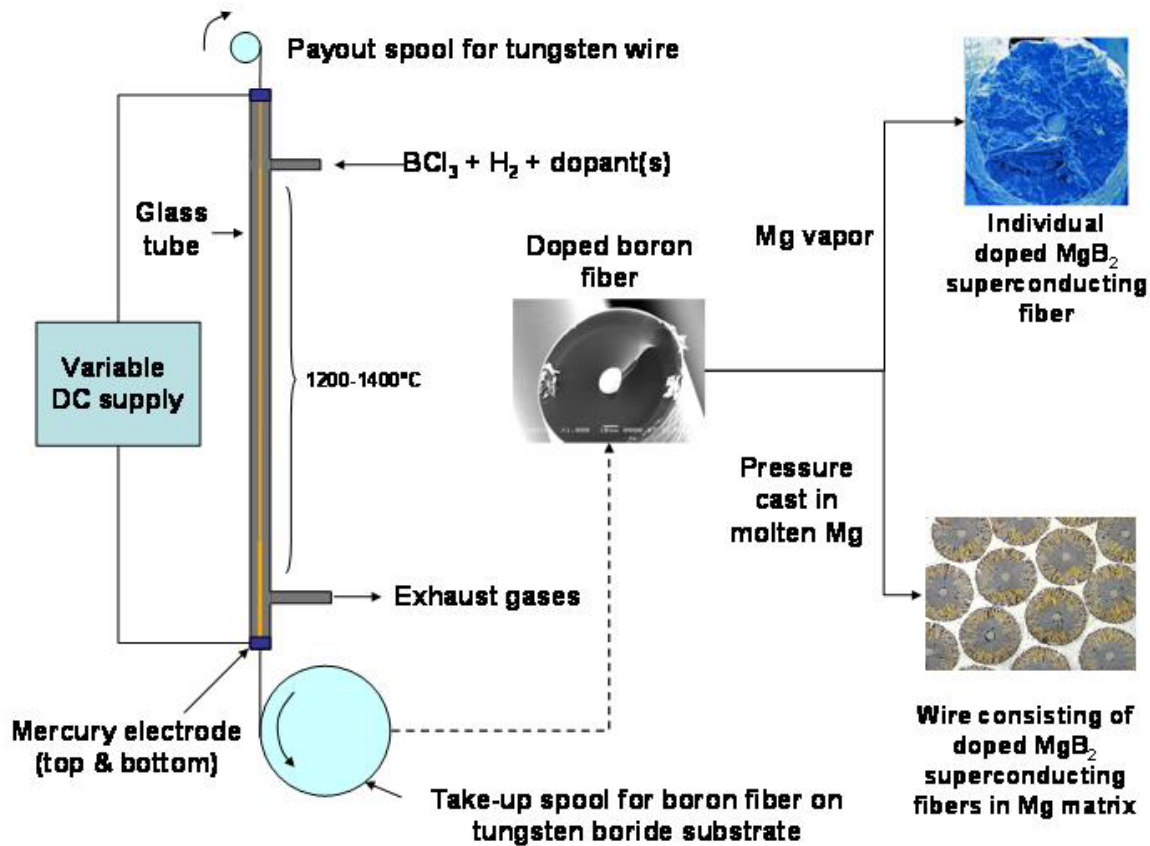


Figure 1. Process diagram showing CVD synthesis of boron fiber [1] and conversion to MgB_2 by reaction with magnesium vapor [3-7, 9] or molten Mg [8]

In a recently reported alternate approach [8], gas phase doping techniques are applied during the formation of boron powders by the reduction of boron trichloride in a hydrogen plasma. Gaseous or liquid moieties containing controlled concentrations of the dopants are injected into the plasma and incorporated *in situ* during the reductive pyrolysis. This process is postulated to achieve dopant dispersion on the atomic scale within the boron particles rather than a coating or a mixture of particles. The resulting powders were then used to fabricate magnesium diboride superconductors in neat pellet form and wire form using the powder-in-tube PIT method (Figure 2).

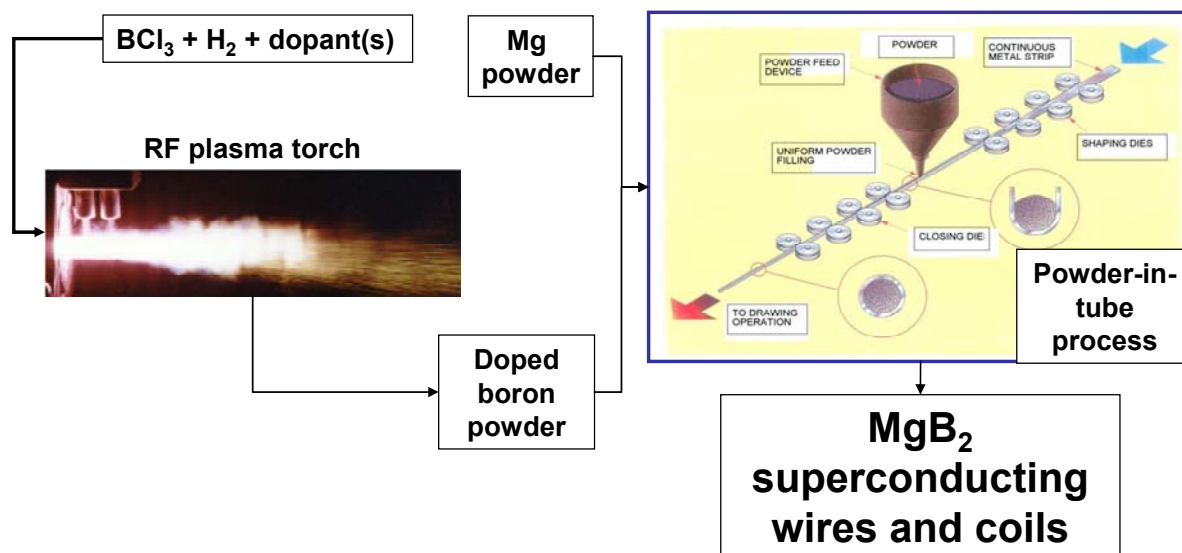


Figure 2. Process diagram for MgB₂ wire from plasma synthesized doped boron powder.

The results achieved in the Phase I STTR Project suggest research and development work which would include the innovative application of chemical vapor deposition (CVD) and plasma synthesis technology to the preparation of enhanced chemically doped boron substrates, their conversion to MgB₂ with improved superconducting properties, and process development to produce continuous MgB₂ wires.

1.1.4 Background

Superconductivity in MgB₂ was first reported early in 2001 [1]. The report generated intense interest for a number of reasons. The material not only showed a superconducting transition temperature significantly above those of the classical “low temperature superconductors” (LTS), but is inexpensive and readily available in powder form. With the discovery of superconductivity in MgB₂ there appeared to be an opportunity to make an important new conductor material for large-scale magnets that operate in the range of 20K. Researchers quickly determined the properties of MgB₂ and showed that it was a “classical” BCS superconductor. Another important property it shares with the intermetallic LTS materials such as NbTi and Nb₃Sn is the ability to carry large currents across crystalline grain boundaries. The reported transition temperature of 39K is approximately twice that of the LTS. The LTS are widely used today in magnetic resonance imaging (MRI) medical diagnostic systems and in large research magnets and require liquid helium temperatures for their operation. The higher transition temperature of MgB₂ would allow operation at temperatures achievable by mechanical closed-cycle refrigeration systems, eliminating the need for expensive liquid cryogenes. The copper oxide perovskite-type “high temperature superconductors” (HTS) have transition temperatures above 77K; however, at low temperatures, the upper critical magnetic field is highly anisotropic

and weak grain boundary coupling makes current densities sensitive to orientation (crystallographic texturing). This makes HTS use in MRI and other magnet applications problematic.

Soon after the discovery of superconductivity in MgB_2 , a group at Ames Lab/Iowa State University reported a method [14] of making superconducting MgB_2 wires from high purity, chemically vapor deposited (CVD) boron filaments that are commercially available from Specialty Materials, Inc. [15]. This method involved sealing the boron filaments in a tantalum tube with excess magnesium and heating at approximately 900°C , causing the magnesium vapor to react with the boron. The $100\mu\text{m}$ boron fibers were converted to $150\mu\text{m}$ polycrystalline MgB_2 wires. Cross-sections of wires made by this method have been depicted on the covers of *Physics Today* [16], *Physics World* [17], and a full-page illustration in *Scientific American* [18] (Fig. 3). Wire segments 5cm long could be isolated. The wires were brittle and fragile compared to the initial boron filaments, but were sufficiently robust to allow measurements. Fully reacted wire segments were consistently found to show critical current densities, J_c , ranging from $1 \times 10^5 \text{ A cm}^{-2}$ to $5 \times 10^5 \text{ A cm}^{-2}$ at magnetic fields in the range of 0.1T with a drop by a factor of about 100 as the magnetic field increased to 3T. The properties of these pure samples are insufficient to be competitive with current materials, but they should be considered lower limits.

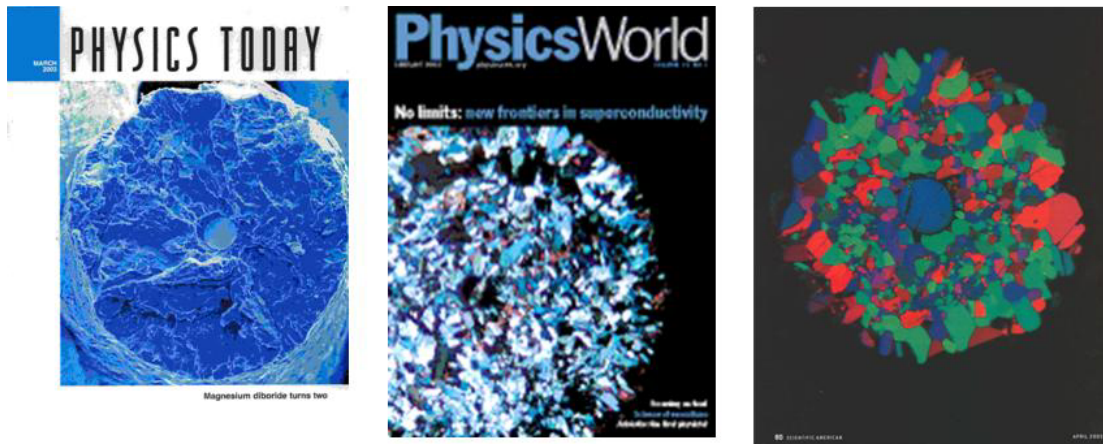


Figure 3. Cover art: MgB_2 made from Specialty Materials boron fiber shown on the covers of *Physics Today* (March, 2003) [10], *Physics World* (January, 2002), and in *Scientific American* (April, 2005).

Magnesium diboride is a Type II superconductor in that conduction in high magnetic fields can be enhanced by the addition of “pinning centers” for the magnetic field lines or vortices. Pinning sites can be grain boundaries or impurity precipitate clusters that locally act like normal conductors embedded in the superconducting medium. Zero resistance in this mixed state can be maintained if the magnetic vortices are restrained from moving. In this case, both the upper critical field, H_{c2} , and the critical current density, J_c , above which resistance develops can be increased substantially. The trade-off is that the transition temperature may be suppressed by the impurity addition. Very successful Ti doping experiments using a solid state reaction method have been reported [11] in which powders of Mg, Ti and B were mixed, pressed and reacted on

an MgO plate in flowing argon gas. The best results were found for a Ti/Mg ratio of 0.1 which showed a $J_c \sim 2 \times 10^6 \text{ A cm}^{-2}$ at 5K and zero field. In this case, the dopant was found to be segregated at the grain boundaries. The next section describes some the initial experiments on the doping of MgB_2 with Ti via a chemical vapor deposition (CVD) route which provided even higher levels of improvement. Also discussed below are experiments in which the boron starting material was doped with carbon by CVD co-deposition. In this case, H_{c2} values were increased to ~ 35 Tesla. Finally, initial experiments to fabricate MgB_2/Mg superconducting composite wires are discussed.

1.1.5 Initial Experiments

Commercial boron fibers are manufactured by a continuous CVD process [15]. **The current price of commercially available 100 μm diameter CVD boron fiber is <5¢ per meter.** In this process, a 12 μm diameter tungsten wire is drawn continuously through a 2 meter long vertical glass reactor which is sealed at the top and bottom by pools of mercury. The mercury forms both an electrical contact and a gas seal. A metered mixture of boron trichloride and hydrogen is admitted to the reactor through a sidearm at the top and spent process gases are exhausted through an outlet near the bottom of the reactor. The wire in the reactor is resistively heated to 1300-1400°C by application of the appropriate voltage to the mercury seals. At the temperature of the substrate, the boron trichloride is readily reduced by the hydrogen; pure, solid amorphous elemental boron is deposited and byproduct hydrogen chloride is exhausted at the bottom of the reactor. The diameter of the boron produced is determined by the drawing rate of the wire through the reactor; a residence time on the order of one minute results in a 100 μm boron fiber (with a reacted tungsten boride core) being spooled continuously at the bottom. Boron fibers produced this way were converted to magnesium diboride wire by the Iowa State process of reaction with magnesium vapor.

The above process was modified to introduce dopants into the boron during its formation. Experiments to systematically introduce dopants into MgB_2 at later stages of processing, e.g. by solid state diffusion, have proven problematic because it is difficult to substitute for Mg or B atoms in an existing MgB_2 lattice. In the CVD route, a dopant can be introduced as a vapor phase reactant which co-deposits with the boron, leading to very fine scale dispersion of the dopant. Concentration can be conveniently controlled through metering the vapor phase concentration.

The doping of MgB_2 with Ti via incorporation into a CVD boron filament precursor [6,7] resulted in homogeneous dispersion of 2-14 nm TiB precipitates throughout the larger MgB_2 grains (Figure 4). The addition of Ti dopants by CVD co-deposition resulted in the homogenous dispersion of precipitates on a very fine scale. The significant improvement in the critical current densities (compared with undoped MgB_2 and MgB_2 doped by traditional solid state methods) can be attributed to enhanced flux pinning from this finely dispersed precipitate phase. At low fields, the plot of J_c for the two doped samples at 5K shows values a factor of 8 higher than that of pure MgB_2 . Above 2T, the improvement compared to pure MgB_2 is very substantial (Figure 6). Ti-doped MgB_2 made from CVD boron fibers show $J_c > 100,000 \text{ A cm}^{-2}$ at a temperature of 20K (Figure 6).

The boron fiber starting material has also been doped with carbon by CVD co-deposition [7]. In this case, upper critical magnetic field (H_{c2}) values were increased to over 30 Tesla (Figure 7). The superconducting transition temperature showed a systematic decrease from

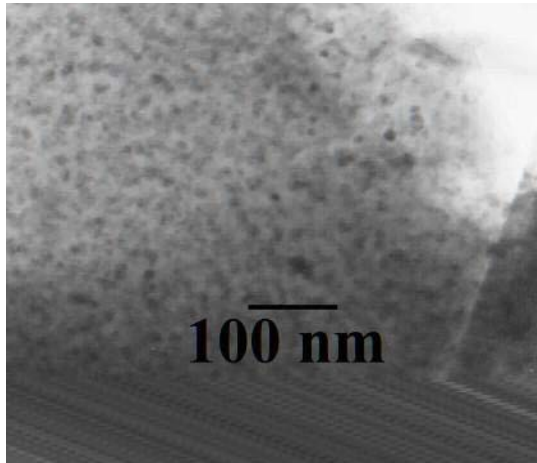


Figure 4. Single crystal of MgB_2 doped with TiB (dark inclusions) [6].

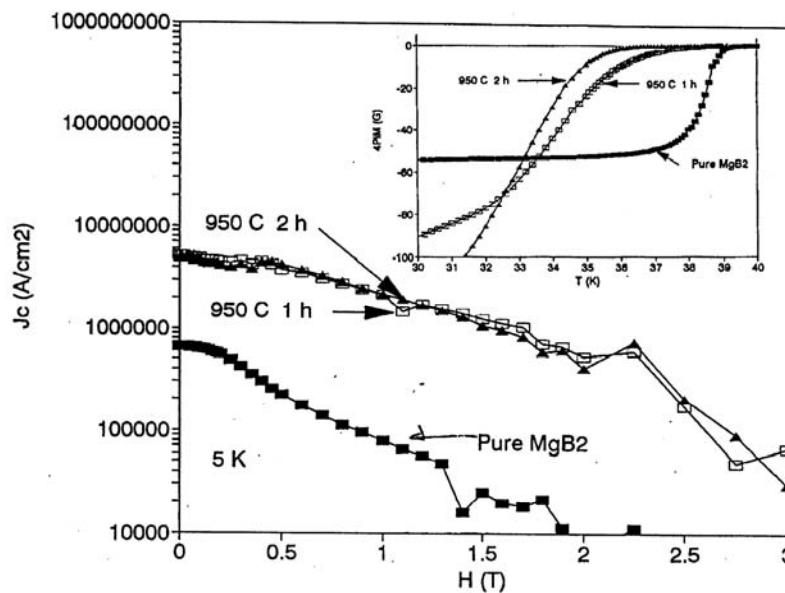


Figure 5. Plot of values of J_c versus magnetic field at 5K for Ti-doped MgB_2 reacted at 950°C [6]. The Ti-doped material shows an order of magnitude or more improvement over undoped MgB_2 . The inset shows magnetization data for these samples.

38.6K to 36K as the carbon concentration increased. The critical magnetic field values were determined in three ways: by resistance vs temperature, magnetization vs field, and by resistance vs field (at the National High Magnetic Field Laboratory). The results are shown in Figure 6. Note the systematic increase in H_{c2} with increasing concentrations of carbon. **Note that H_{c2} for MgB_2 -3%C exceeds that of Nb_3Sn at all temperatures and is among the highest seen in any bulk sample of MgB_2 .** Furthermore, the results suggest that the optimum concentration of carbon in order to maximize the value of the upper critical field has not yet been achieved.

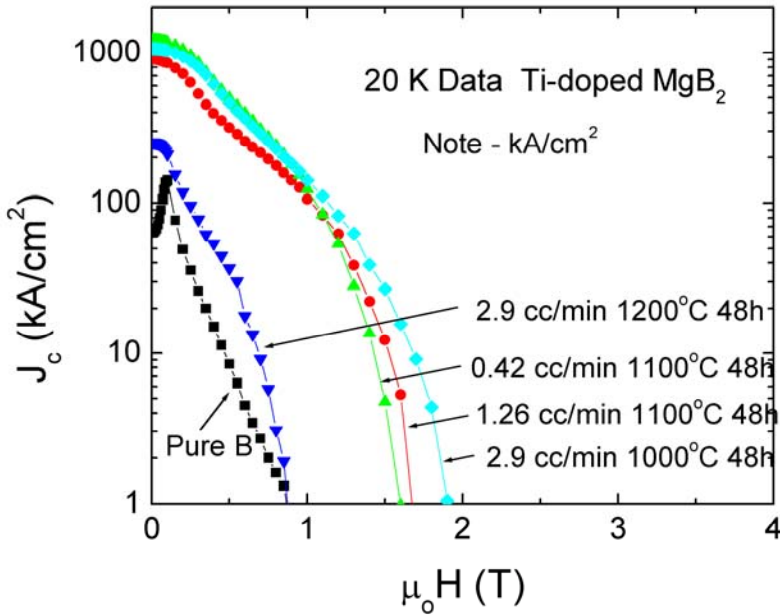


Figure 6. Critical current density vs. magnetic field at 20K for Ti-doped wire samples made from CVD boron fibers [7]. The data at 1100°C shows a monotonic increase in J_c with increasing dopant at higher magnetic fields. Processing at 1200°C nullify the benefits of doping presumably by a coarsening of the grain structure.

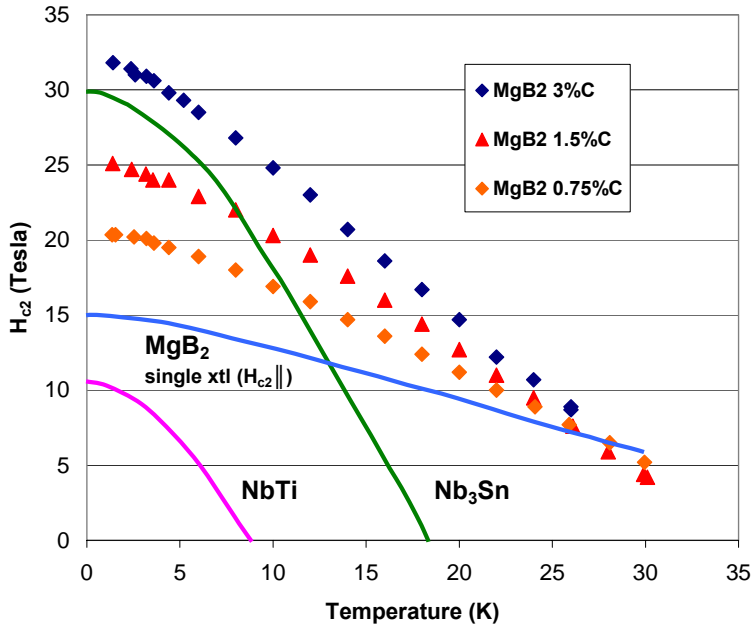


Figure 7. MgB_2 made from doped boron fiber; plot of the upper critical field, H_{c2} , as a function of temperature shown for three atomic doping levels of carbon into MgB_2 [5]. Note that H_{c2} for MgB_2 -3%C exceeds that of Nb_3Sn at all temperatures.

The work described in the previous paragraphs demonstrates that by co-deposition via a CVD route, dopants can be introduced as vapor phase reactants that co-deposit with the boron, leading to very fine scale dispersion of the dopant. Concentration can be conveniently controlled through metering the vapor phase concentration. **This demonstrates that doping by gas phase synthetic techniques can provide significant improvement over current state-of-the-art powder methods for doping MgB_2 .**

1.1.6 Liquid Metal Reaction

Initial work the STTR Research Institution P.I. (Dunand) suggested that the fabrication of MgB₂/Mg composites by reactive liquid metal infiltration technique [13,19,20] is worthy of further investigation as a technique for the fabrication of superconductor wires. The brittle and hygroscopic nature of MgB₂ fibers makes it interesting to produce a composite consisting of an intimate, small-scale mixture between the superconducting MgB₂ fibers and a tough, metallic phase. This work was the first to investigate synthesis of MgB₂ without vapor phase transport, by direct reaction of solid B with liquid Mg. As compared to gas-phase synthesis, the flux of Mg atoms to the B surface is much higher, possibly accelerating the kinetics of MgB₂ formation. Using excess Mg allows for the creation of composites. Furthermore, near-net shape casting can lead to objects with tight dimensional tolerance, and **the process can be scaled up to become continuous, e.g., for wires** [21]. The liquid route is further attractive because Mg has a low melting point (650°C).

Initial work [19] in the Mg-B system demonstrated that amorphous B powders could be reacted very rapidly with excess quantities of liquid Mg, thus forming an Mg/MgB₂ composite. The B powders (4-44µm in size) were first compacted into a preform which was pressure-infiltrated with liquid Mg at 700°C. Partial synthesis of MgB₂ was observed after infiltration, and could be completed by annealing at 950°C for two hours, as shown by x-ray diffraction (XRD). This was the first publication demonstrating that synthesis with liquid Mg was a viable, and indeed promising, process route for MgB₂ and its composites.

The liquid infiltration concept was further extended [13] to the case of continuous B fibers (with a diameter of 140µm, and a 15µm tungsten boride core), which were aligned in a bundle within a steel crucible, and pressure-infiltrated with liquid Mg at 800°C. The composite was then annealed at 950°C for two hours under argon pressure. Complete reaction occurred between the B fibers and the liquid Mg, resulting in MgB₂ fibers in a pore-free Mg matrix. The cross-section

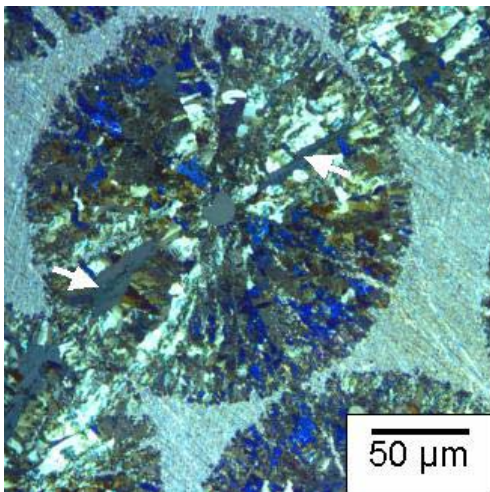


Figure 8. Optical micrograph of fully reacted 200µm MgB₂ fiber in Mg matrix under cross-polarized light (original B fiber was 140µm in diameter). Arrows indicate slivers of non-birefringent material (un-reacted B). A 15µm W-B core (from the original B fiber) is located at the center of the MgB₂ fiber. The interface between the matrix and fiber is well bonded.

of reacted fibers exhibited birefringence when observed under cross-polarized light (Fig. 8), a characteristic of bulk MgB₂. Secondary-ion mass spectroscopy (SIMS) measurements showed the presence of both Mg and B within the fibers. Direct proof of MgB₂ synthesis was provided by XRD analysis of crushed composite powders, showing only Mg and MgB₂ peaks.

Additionally, an extracted fiber was found to be superconducting at a critical temperature slightly above 39K (Fig. 9), in good agreement with the value of 39K for bulk MgB_2 [1]. The critical current density of that fiber was determined under zero field conditions as $3.6 \times 10^5 \text{ A cm}^{-2}$ at 5K and $2.1 \times 10^5 \text{ A cm}^{-2}$ at 20K. Nearly the same values were found for free-standing MgB_2 fibers synthesized by reaction of B fibers with Mg vapor [14]. Optimization of our process through alloying or change of processing variables (e.g., heat-treatment temperature and time) to create pinning centers (e.g., grain boundaries and impurities) will probably lead to higher current densities [11,22,23], which will need to be confirmed by transport J_c measurements.

Unlike the irregular shape of the MgB_2 fibers produced by reaction in gaseous Mg, the present MgB_2 fibers created by reaction with liquid Mg retained their original cylindrical shape. Most of the fibers extracted by dissolution of the matrix had the same length as the composite specimen piece being dissolved (9mm) and were straight. This was probably due to the much more uniform flux of Mg atoms provided by the Mg melt in direct contact with the B fibers, allowing a uniform diffusion front within the fibers, and thus a uniform volume expansion.

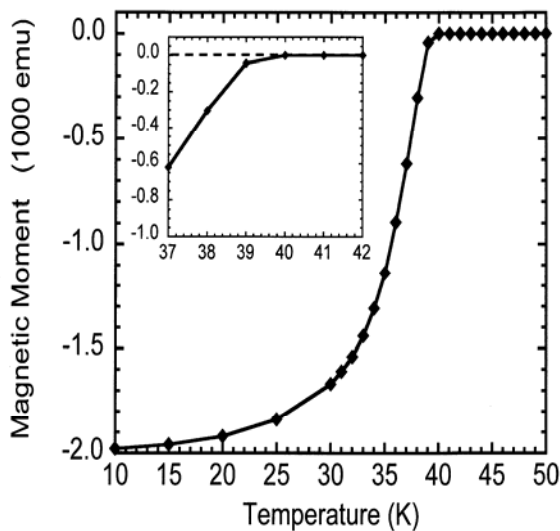


Figure 9. Magnetic moment versus temperature under zero field conditions for single MgB_2 fiber extracted from the reacted composite. Inset shows T_c slightly above 39K as measured with a superconducting magnetometer.

However, this volume expansion ($\Delta V/V=0.86$) was also probably responsible for radial cracks observed for most fibers. The cracks were filled with magnesium, which indicates that they formed during synthesis from the volumetric change, and not upon subsequent cooling from the mismatch in thermal expansion between Mg and MgB_2 . Also, most MgB_2 fibers contained unreacted B in small, isolated radial slivers, which were visible under cross-polarized light (Fig. 8), but with a volume fraction too low to be measurable by XRD. These slivers were on average $10\mu\text{m}$ wide and $40\mu\text{m}$ long. Finally, the fiber/matrix interface appears well bonded, of importance for the mechanical properties of these composites. In a later experiment, B fibers with $100\mu\text{m}$ diameter were reacted for 1.5 h at 950°C . Fig. 10 shows that partial reaction has occurred, with a shell of MgB_2 surrounding the unreacted central portion of the B fiber. This picture illustrates that the reaction occurs by solid-state diffusion of Mg or B through the MgB_2 shell, and that a defined, but somewhat irregular, reaction front travels radially through the fiber. Short cracks are also visible within the MgB_2 shell.

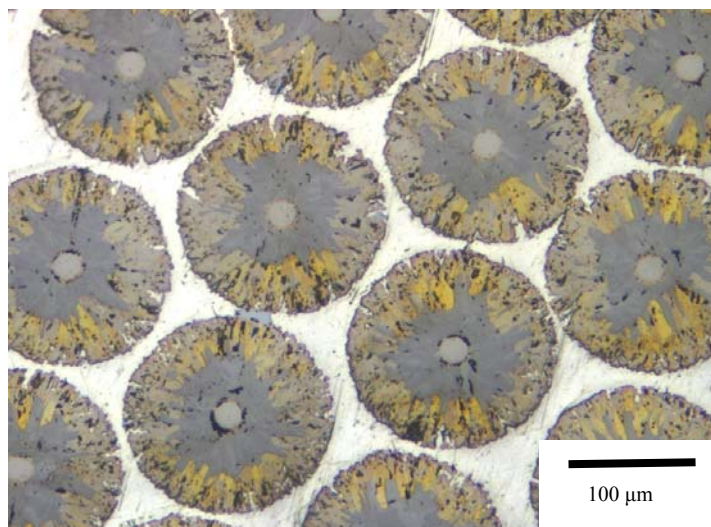


Figure 10. Optical micrograph of partially reacted MgB₂ fiber in Mg matrix (original B fibers were 100μm in diameter). An outer shell of MgB₂ (yellow) has propagated radially and is in contact with an inner core of unreacted B (gray). The interface between the Mg matrix (white) and fibers is well bonded.

1.1.7 Boron Powder Synthesis

The availability of boron of known and controlled composition is a key factor in the development of MgB₂ superconductors. As noted above, CVD boron filaments can be synthesized with 5 9's purity, and controlled concentration of dopants can be added with uniform dispersion. The most common route to MgB₂ superconducting material is the synthesis of MgB₂ powder by the direct chemical reaction between powders of elemental boron and magnesium. Commercial boron powder is manufactured by the magnesiothermic reduction of boron oxide. Typical purity ranges from 91-97%. High purity grades (~99%) are available only at high cost. Dopant additions to MgB₂ are typically carried out by solid state reaction methods during MgB₂ synthesis, with varying results with respect to concentration and dispersion.

During the course of the Phase I project, research at Specialty Materials in conjunction with several collaborators made it increasingly clear that there was another promising path to doped MgB₂ superconductors. It involves the synthesis of nano-sized boron powder by the hydrogen reduction of boron trichloride in a plasma [24], which offers the opportunity for both high purity and controlled dopant addition. Specialty Materials, Inc., funded work with the Center for Thermal Spray Research at the State University of New York at Stony Brook to produce nanoparticle boron powder by axially injecting a BCl₃/H₂ gas mixture into an RF coupled plasma. The apparatus (Figure 11) is designed to allow collection and packaging of the powder without exposure to air in order to minimize contamination. These efforts have demonstrated the capability to synthesize sub-micron boron and doped boron powder (Figure 12). A major advantage of this technique lies in an extension of the CVD doping method described above. Addition of gaseous dopant precursors to the reactant gas stream in the plasma is expected to produce uniformly dispersed dopant. The risk in this approach lies in the extreme reaction conditions in comparison with the CVD conditions used previously, and the fact that the plasma process requires gas phase nucleation, which may be influenced by the dopant. These

risks are not considered prohibitive. Although extreme, the plasma reaction is inherently a CVD process with the accompanying latitude in gas flows, pressure, reactant composition, gas residence time, and power levels. The combination of these factors should provide control over nucleation and the dopant concentration in the powder product. Initial experiments to synthesize carbon-doped boron nanopowder showed much promise and warrant further investigation.

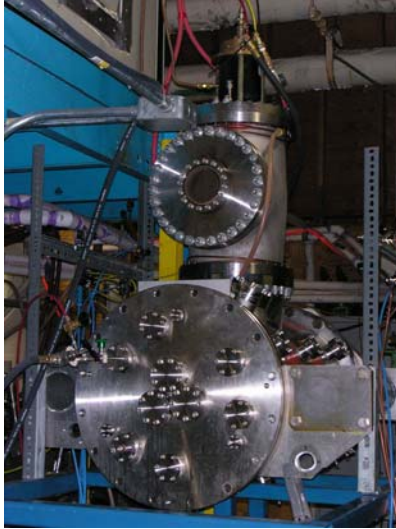


Figure 11. Chamber used for RF plasma synthesis of pure and doped boron nanopowders.

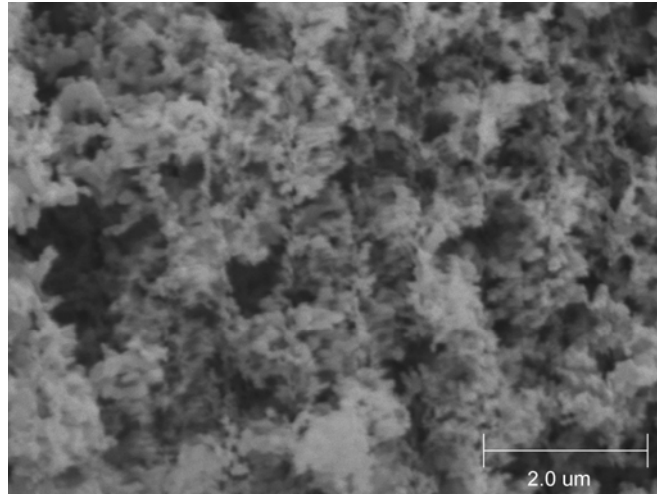


Figure 12. Sub-micron boron powder produced via a plasma synthesis technique by the collaboration of SMI and SUNY at Stony Brook.

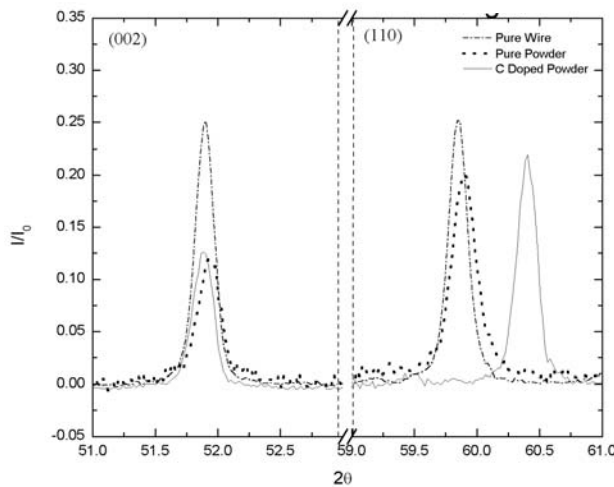


Figure 13. X-ray diffraction patterns (Cu K_{α} radiation) of MgB_2 made from pure and doped plasma synthesized boron powder; the a-axis shift of the (110) peak [8] corresponds to approximately 7.4% carbon substituted into the MgB_2 lattice.

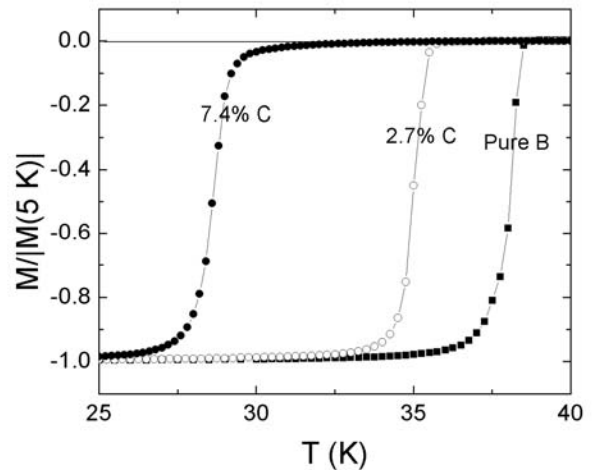


Figure 14. Properties of MgB_2 made from plasma synthesized carbon-doped boron powder showing T_c vs atomic % C

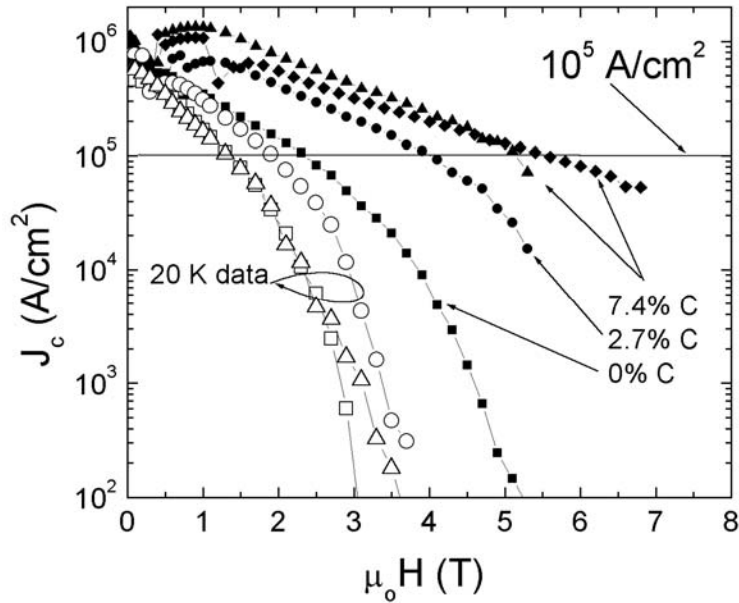


Figure 15. Critical current density vs field at 5 K (solid points) and 20K (open points) of carbon-doped MgB_2 made from plasma synthesized carbon-doped boron powder [8]

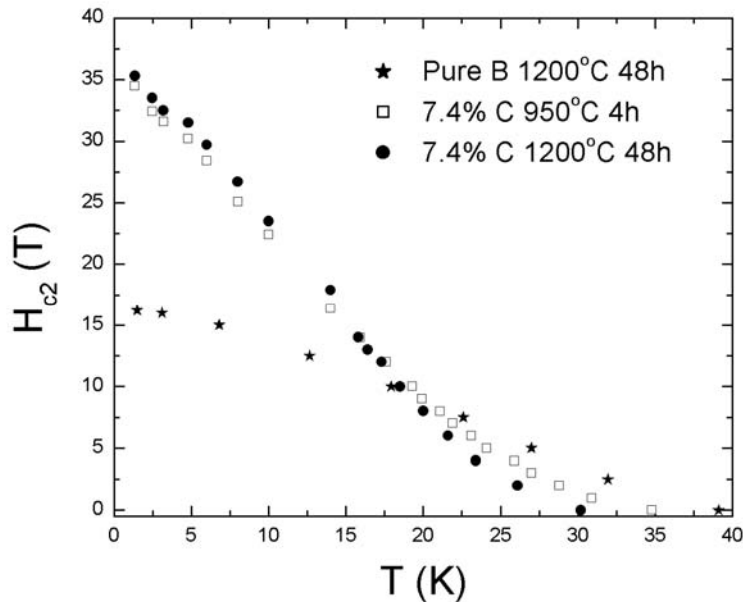


Figure 16. Upper critical magnetic field data [8] for samples prepared from C-doped boron powder showing $H_{c2}(T=0) \sim 37$ tesla, the **highest value seen to date for MgB_2 bulk materials**

Specialty Materials' collaborators at Ames Lab reacted the doped powder with Mg vapor to form MgB_2 . A gas stream of approximately 5 liters/min H_2 , 3 liters/min BCl_3 , and 60 cc/min CH_4 injected into a plasma torch produces boron powder composed of 5 to 50 nm particles of carbon doped boron powder that agglomerates into structures of micron size that look like lace in the scanning electron microscope. The gas flow ratio gives a nominal 2% C content. These C-doped B powders can then be reacted to C-doped MgB_2 in a Mg vapor either in the form of loose powders, pressed pellets, or PIT conductors. An X-ray study of these powders with Cu K_α radiation shows that the a-axis shift of the (110) corresponds to approximately 7.4% C [8] as illustrated in Figure 13. This shows that the carbon deposition is very efficient and actually gave a higher content than originally planned. Similar analysis showed that a gas flow ration of

1% carbon in the plasma synthesis process resulted in a 2.7% concentration of carbon in MgB₂ as indicated by x-ray diffraction. The plot of Figure 14 shows T_c vs %C.

Pressed pellets of the 7.4% carbon material were taken to the National High Magnetic Field Laboratory at Florida State University for resistivity vs magnetic field measurements. The carbon-doped MgB₂ showed J_c > 100,000 A cm⁻² out to 5-6 Tesla at 5K and out to nearly 2 Tesla at 20K (Figure 15). H_{c2}(T=0) values were ~ 37T (Figure 16). The superconducting properties of carbon-doped MgB₂ using Specialty Materials' carbon-doped boron powder **are comparable to the best results yet reported for bulk MgB₂ superconductors**. It should be noted that this data is prior to a full optimization of processing parameters or dopant concentrations.

1.1.8 Powder-In-Tube (PIT) Wire Processing

A promising path toward achieving low-cost MgB₂ superconducting wire is the powder-in-tube (PIT) method [25,26]. Wires made by PIT processing from plasma synthesized boron nanopowder will be pursued in parallel with the liquid infiltration method of fibers described above. In MgB₂ produced by the PIT process, the quality of the superconducting wire is limited by the quality and purity of the powder reactants. Small particle size, high surface area powder is also desirable to increase reaction rate with Mg and decrease the grain size of the MgB₂ product. Appreciable quantities of high purity, high surface area boron powder is especially difficult to obtain. The purity of the boron powder used for the fabrication of MgB₂ wires typically is in the range of 93-99%. The presence of undesired impurities has been shown to lead to weak-link behavior thus reducing the critical current of MgB₂ [25]. Boron powder with purity 99% or greater is at present available in limited quantities and at high costs. Furthermore, users of boron powder [27] have estimated that the current supply of high purity (≥ 99%) amorphous boron will be exhausted sometime in the year 2005. A pure, nano-sized, amorphous boron powder would not only function as a raw material for the synthesis of pure and doped MgB₂, but would also serve the larger chemical community as a material for any chemical synthesis or process requiring pure, high surface area boron powder. This proposal outlines an overall research and development plan which includes the innovative extension of CVD technology to the plasma synthesis of chemically doped boron nanopowders, and their conversion to MgB₂ with improved superconducting properties.

In the PIT method, powder, in either reacted or unreacted form is encapsulated in a metal sheath, which can be sealed by a number of methods. The sheathed powder typically undergoes a heat treatment in order to further react and/or sinter the material. Subsequent processing includes drawing, shaping, and winding the final wire or ribbon material. In contrast to the higher temperature superconducting oxides (e.g. YBCO, BSCCO), which exhibit weak-link behavior across grain boundaries, MgB₂ seems to be more amenable to a wider range of powder processing techniques. Several workers [27-31] have used the PIT method to produce MgB₂ superconducting wires exhibiting high critical current densities at moderate magnetic fields. Typical sheathing materials include iron, copper, and tantalum. Several workers have shown that critical currents in excess of 1 x 10⁶ A cm⁻² are achievable at 4-5K and zero field; however, these values typically drop off rapidly with increases in temperature and magnetic field. Recent reports [12] have indicated that the critical current performance of PIT

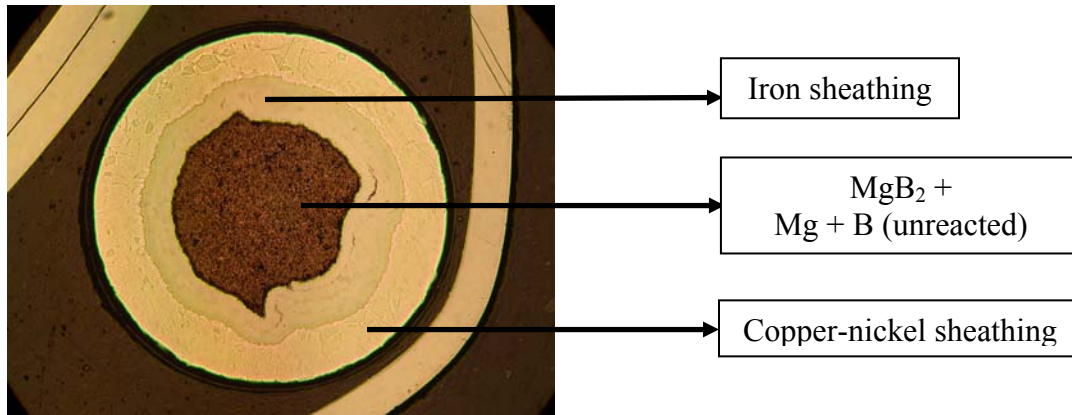


Figure 17. Optical micrograph of a polished cross section of a superconducting wire formed by the powder-in-tube (PIT) method. In the wire pictured here, Specialty Materials carbon-doped boron nanopowder was reacted with Mg at 900°C for 20 minutes.

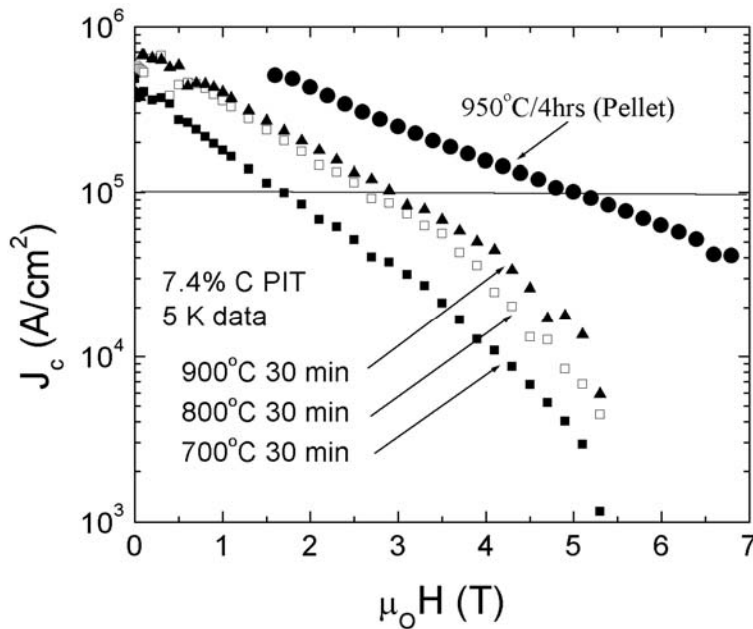


Figure 18. Comparison of 5K critical current density data (J_c) for wires reacted at different temperatures for 30 min [8]

wires of MgB₂ can be increased at higher fields by the addition of dopants. Dou et al [9] has reported J_c in excess of 10^5 A cm⁻² at 20K and 2T in SiC-doped MgB₂. A wide variety of other materials have been introduced into MgB₂ to enhance flux pinning including TiB₂ [11], YB₄ [10], and Mg₂Si [12], and all of these seem to produce substantial increases in the critical current density, J_c , for magnetic fields in the 5-10T range. For most of the efforts to fabricate practical conductors, the PIT method has been used in which it is desirable to have very uniform and small powder particles so that the reaction times will be short and the grain size will be small to get the advantage of grain boundary pinning.

Carbon-doped Specialty Materials' boron nanopowder has been fabricated into MgB₂ superconducting wires in collaboration with Hyper Tech Research, Inc. A cross section of a one

of these wires is shown in Figure 17. Figure 18 shows the superconducting properties of a PIT wire made from C-doped boron nanopowder. Work is in progress to determine the extent of porosity and the fraction of MgB₂ vs other borides in the superconducting core. The PIT process offers a viable established route for the formation of continuous MgB₂ superconductors. A number of investigators have demonstrated good superconducting properties in cable form, typically achieving 50% of the properties of the same material processed in neat form. Doping of the MgB₂ to increase J_c and/or H_{c2} will be required to make MgB₂ clearly advantageous over existing superconducting materials. As doped boron powders become available in this program, the PIT process offers a fast route to measure the performance characteristics of MgB₂ superconducting wire based on plasma synthesized boron nanopowders and in the longer term (e.g. in a more extensive development program such as a Phase II SBIR program) a fast route to the availability of continuous MgB₂ superconductors for fabrication of prototype components and end-user evaluation.

1.2 Anticipated Public Benefits

The potential benefits of successful development of superconducting MgB_2 wire and the growth of this market will be broad based across all of society. Fusion research will lead us to a new and exciting energy source. Fusion fuels are in abundant supply and available around the world. Equally important, fusion energy can generate electricity without producing greenhouse gases which contribute to global warming. Moreover, the radioactive wastes that are generated have very short half-lives, thus eliminating long-term storage problems. However, in order to harness fusion as a practical energy source, many significant technical challenges must be overcome. Key among them is developing superconducting coils of unprecedented size (for containment and control of the plasma in magnetic confinement fusion), which are cost effective to fabricate and operate. While conventional and LTS magnets are options, MgB_2 superconducting magnets operating around 20K with their ability to carry very high current densities at high fields offer an exciting alternative.

Specific groups in the fusion area that could benefit from the development of MgB_2 magnets include the International Thermonuclear Experimental Reactor (ITER) and the Spallation Neutron Source (SNS). Both are key projects for proof of concept and development of fusion energy. It is projected that ITER would require 517 tons of Nb_3Sn and 244 tons of $NbTi$, since only these materials can currently achieve the necessary high field strength and precise control of magnetic field. The SNS project is part of the DOE's effort to advance the technology of fusion energy. Development of doped MgB_2 with potentially lower cost per mass and cost per length than existing LTS materials could reduce cost and increase the odds of a future commercial fusion reactor.

In addition to these applications, MgB_2 could be used for very large magnets required in the study of high energy physics to focus and bend particle beams in accelerators. Advances in accelerator magnet technology could lead to more widespread use of particle accelerators in the treatment of cancer patients [32]. Peter Limron, head of the technical division of Fermilab stated, "The promise of MgB_2 is that it is a potentially inexpensive superconductor that can operate at elevated temperatures, thereby simplifying costly and complex cryogenic systems. This may lead to capital and operating savings for large colliders and other accelerators and, possibly more important, could lead to greater reliability and availability." [17]

Health care will also be dramatically affected both in terms of cost and quality of service. Although demographic trends such as greater numbers of older people due to longer life expectancies have contributed significantly to rising costs, the inability to quickly, accurately and cost-effectively diagnose diseases with current equipment is a major cost driver. The widespread use of less expensive and higher precision MRI units, enabled by the use of MgB_2 magnets could have a profound effect on reducing both health care costs and suffering by providing earlier diagnosis.

Specifically, use of MgB_2 magnets could speed up the trend of more powerful, smaller, more efficient and more affordable open MRI systems. The resulting benefits to the patient include eliminating the need for harmful x-ray examinations and exploratory surgery. These systems can provide real-time imaging during surgery, and reduce the discomfort of patients. Corollary benefits include shorter hospital stays and reduced medical staff, two primary drivers in the ever increasing costs of health care.

Additionally, the large scale and widespread power outage along a large portion of the east coast two years ago demonstrated how dependent we are upon a safe and extremely reliable power grid. Given the strong correlation between energy consumption and gross domestic product, there exists a steadily increasing demand for power. This has the potential to overwhelm the capacity of some aging power grid infrastructures, much like what happened in the Northeast. MgB₂ wire could make energy transmission more efficient and reliable and hence could dramatically improve these situations.

An economic study comparing MgB₂ with LTS and HTS materials conducted by P. Grant (Presented at the Materials Research Society 2001 Fall Symposium E, Materials for High Temperature Superconductor Technologies, E1.1) when he was employed by EPRI (Electric Power Research Institute) helps to demonstrate the potential financial benefits associated with MgB₂. Two such results are presented in Tables 1 and 2 which compare the cost/performance and cost of ownership respectively of various superconducting materials. In both cases MgB₂ is very attractive. Since the appearance of the Grant work, SMI in conjunction with Iowa State University has demonstrated further improvement in the superconducting properties of MgB₂ by selective doping and thus MgB₂ looks even more attractive.

Specific groups within the commercial sector who would benefit from a fully developed MgB₂ superconductor would include the equipment manufacturers for each of the specific applications. MRI manufacturers such as GE Medical Systems, Phillips, Marconi, Siemens, Hitachi, and Toshiba could build smaller and more efficient MRIs. This, in turn, would flow benefits to MRI customers (hospitals and clinics) who could provide better and more reasonable diagnostic care. Power utility applications manufacturers include GE Power Systems, Alston, Siemens, and Mitsubishi for power utility generators; General Dynamics and Rockwell for ship motors; Siemens ABB and General Atomics for transformers; and General Atomics for fault current limiters.

Table 1
Comparison of the Cost/Performance (C/P) of several LTS and HTS wire technologies
(Presented at the Materials Research Society 2001 Fall Symposium E, Materials for High Temperature Superconductor Technologies, E1.1)

<u>Wire</u>	<u>C/P (\$/kA×m)</u>
NbTi (4.2K, 2T)	0.90
Nb ₃ Sn (4.2K, 10T)	10
BSCCO (25K, 1T)	20
YBCO (25K, 1T)	4
MgB₂ (25K, 1T)	1

Table 2
Cost of ownership of wire specification for several conducting materials in temperature and magnetic field relevant to transformer applications.

(Presented at the Materials Research Society 2001 Fall Symposium E, Materials for High Temperature Superconductor Technologies, E1.1)

Item	Units	Cu	BSCCO	YBCO CC	MgB₂
Total Cost of Ownership	\$/kA×m	65	80	85	<u>59</u>

The specific products resulting from this STTR development program would be MgB₂ wires and/or powders. While HTS materials have been under development longer, they are fraught with technical and economic problems which are preventing their growth and replacement of conventional LTS materials such as NbTi and Nb₃Sn. Although MgB₂ wire has been drawn and evaluated, the starting MgB₂ powder has not been optimal in that desired dopants which improve current carrying capacity and upper critical field have not been present with uniform distribution.

Specialty Materials has demonstrated two paths to doped MgB₂ which enhance the properties over baseline materials. As the technical program develops, one of these two processes (MgB₂ wire converted from doped boron fibers cast in Mg, or the plasma synthesized doped boron powder converted to MgB₂ wire by powder-in-tube processing) will represent the better product from a cost/performance perspective. Either of these products represents an advantage over current materials systems. Compared to conventional LTS materials such as NbTi and Nb₃Sn, the doped MgB₂ products have potentially lower operating costs and are lower density.

The other competitive system is HTS wires. Within this system there are two materials of interest, BSCCO, and YBCO. While there are numerous companies in various stages of development for these materials, American Superconductor is viewed as the leading developer of HTS wire based upon YBCO. Although they have demonstrated an ability to make HTS wire, they have not made substantial lengths, and they are forced to rely upon expensive silver cladding to make the wire stable. By their own admission, their product is still several years away, and it is not clear if they will ever be able to produce an inexpensive wire to take advantage of the higher temperature superconductivity of YBCO. Sumitomo Electric claims to be able to mass produce a BSCCO wire capable of transmitting 130 times the electricity carried by conventional copper wire. They have built a production facility in Osaka, Japan, and expect to be selling the wire later this year at a price no more than five times the cost of conventional wire. While this is a promising development for superconductor technology, it remains to be seen if Sumitomo can achieve these lofty goals.

There are several reasons why we believe that our product(s) will be successful in the marketplace. In addition to the technical and cost advantages of doped MgB₂ wire over other material systems, we feel that one of Specialty Materials' advantages is its use of strategic partners. Briefly stated, we are concentrating on our core competence (gas phase processing) and partnering with others who can make wire and manufacture coils for MRI units and other superconducting applications. Other strengths include our experience with making boron fiber

(much like wire), and a capital infrastructure with the capability of making over 2 billion linear feet annually. With current manufacturing of fiber below capacity, we could ramp up to make a starting material for MgB₂ wire very easily without major investment in additional equipment.

Our investment strategy will depend upon whether the doped boron powder or the doped boron fiber proves to be the best approach. Assuming the doped powder route is chosen, we anticipate that a pilot plant induction plasma unit would cost \$300-500 K. This would allow us to produce 2-5 lbs. of powder per day. At some point, we would need to assess the value of converting to a DC plasma furnace, since this would be significantly more cost effective. Further, DC plasma furnaces could be added as required, since there is no economies-of-scale advantage to adding larger units. Adding individual units would allow us to invest only as the market demand requires, plus provide us with manufacturing flexibility.

Should the doped fiber approach be the chosen route, we would not need to make any significant investments until there is a substantial business. We are currently utilizing less than a third of our fiber manufacturing capacity, so we would be able to produce over 15,000 lbs. of doped boron fiber, based upon current utilization. As the business develops further, adding additional reactors to make more fiber is a small expense that can be made incrementally.

A complete analysis of the market for this product will be presented in the Commercialization Plan section (2.7). The following section will demonstrate the significance of the market for this product by presenting a pricing strategy. Since we have two technical approaches to this problem, there need to be two potential pricing strategies. Table 3 shows projected costs of various superconductor wire materials in \$/kA-m, based upon information from Mike Tomsic at Hyper Tech Research, a manufacturer of superconducting wire. As can be seen from this table, MgB₂ represents the best value among all the potential superconducting wire materials. This is also consistent with the cost benefit analysis done by Paul Grant at EPRI and referenced in an earlier section, and more recently an analysis by Lance Cooley et al [33].

Table 3
Cost of Various Conducting Materials (\$ per kA-m)

Source: Hyper Tech Research

Room Temperature Copper	\$10-20
 (The following are at 1 Tesla at 20-30 K)	
Magnesium Diboride (2005)	\$ 1-2
BSCCO 2223 Tape (2005)	\$20-30
BSCCO 2212 Tape (2005)	\$5-10
YBCO coated conductor (in 2008?)	\$2-3

The pricing estimates for MgB₂ assume a starting boron powder cost of ~\$300/lb. at 99% purity. If a lower purity boron powder (95-97%) is used, the cost is only \$120/lb., but that results in a lower critical current density, J_c. Based upon our own cost projections, we believe we can make doped boron powder using the plasma synthesis approach and sell it for \$400/lb. While this is higher priced than the 99% pure boron powder at \$300/lb., the doped boron powder would have a much higher J_c, thus representing a much better value.

Assuming we arrive at the doped boron fibers route, the final wire product would result from continuous casting of the boron fiber in Mg, followed by conversion to MgB_2 . Our projections for that approach show the fiber portion of that cost would be less than \$0.50/kA-m. Adding the cost of continuous casting would bring the completed MgB_2 wire cost at under \$1/kA-m. The rationale for these pricing strategies combines bringing added value to the customer and allowing Specialty Materials to earn a sustainable return on investment.

Estimating magnitude and timing of projected sales for a product that does not yet exist always requires some assumptions. In our case, we have relied upon the business plan of Hyper Tech Research for MRI units. They assume a \$70M business in MgB_2 for MRI units by 2009. This translates to roughly 40,000 lbs. of boron powder. Assuming a selling price of \$400/lb for the boron powder, one arrives at a doped boron powder sales volume for MRI units in 2009 of \$16M. While many variables could affect this number either way, this indicates that a viable business could be achieved in less than five years in this one area. This would create a sound business base which could readily support other areas such as the fusion market.

1.3 Degree to which Phase I has Demonstrated Technical Feasibility

Technical feasibility has been demonstrated in the Phase I project in the following ways:

- The use of CVD boron fiber as a raw material for the fabrication of high field MgB_2 superconducting wires has been demonstrated.
 - o Undoped CVD boron is 99.99+% pure; thus undesired impurities are not a factor
 - o CVD boron can be doped with C, Ti and other dopants in the gas phase resulting in ultra-fine dispersion and controlled concentrations
 - o Composites made by liquid metal infiltration using C-doped boron fiber possessed superconducting properties comparable to those reported for C-doped MgB_2 in which C-doped boron fiber was reacted with Mg vapor. (upper critical field, $H_{c2}(0) > 30\text{T}$)
- Liquid infiltration has been demonstrated as a feasible method to make MgB_2 superconductors from both boron fiber and boron nanopowder.
 - o Kinetics of the $\text{Mg} + \text{B}$ reaction was investigated using both doped and undoped boron
 - o Initial work was carried out to investigate the mechanism of the $\text{Mg} + \text{B}$ reaction in the presence of carbon dopant.
- Plasma synthesized boron nanopowder (~99% pure when undoped) was investigated as an alternative raw material for the fabrication of high field superconducting wires
 - o MgB_2 made with C-doped boron nanopowder exhibited $J_c > 10^5 \text{ A cm}^{-2}$ and $H_{c2}(0) \sim 37\text{T}$ (the highest value of H_{c2} yet reported for bulk MgB_2 superconductors)
 - o Superconducting wires were fabricated from doped and undoped boron nanopowder using powder-in-tube (PIT) methods.
 - o Superconducting MgB_2/Mg composites were made by liquid metal infiltration from doped and undoped boron nanopowder.

1.3.1 Fabrication of Doped Boron Fibers by CVD

As described in a previous section, the B fibers used here were synthesized using a modified commercial CVD process [15]. Carbon-doped and titanium-doped B fibers were prepared similarly to undoped B fibers described above, with the addition, respectively of methane or TiCl_4 to the BCl_3 and H_2 reaction mixture. In C-doped boron fibers, the composition (atomic %) of carbon in the gas mixture relative to boron was 0.5, 1.0, 1.4, 2.0, and 3.0%. In Ti-doped boron fibers, the composition (atomic %) of titanium measured by SEM/EDS analysis was 0.6 and 1.0%. Continuous lengths of 80 μm diameter C-doped and Ti-doped B fibers were produced.

1.3.2 Liquid Metal Infiltration of Boron Fibers

Composite samples were prepared according to a previously established method [13] using doped and undoped boron fiber and magnesium metal. Fibers were cut to 20 mm lengths and bundled into an aligned preform within a 4.5 mm inner diameter titanium crucible. Magnesium cylinders were placed on top of the preform of aligned fibers. The crucible was

introduced into a pressure infiltration furnace where it was heated under vacuum to 800 °C and held for 30 min. to ensure melting of the magnesium creating a seal above the fiber preform. The pressure was then increased with Ar gas to 3.2 MPa in 2 min. forcing the liquid Mg into the evacuated space between the fibers. The composite was cooled under pressure and removed at room temperature. The Mg/B composites were machined from the titanium and a section cut and placed into a Ta crucible with excess Mg. The Ta crucible was sealed in a welded carbon steel capsule. The capsule was placed in a custom vacuum furnace where it was heated under vacuum for the desired reaction time and temperature (e.g. 1000 °C, 96 hr for carbon-doped boron fibers). After reaction, the capsule was quenched in water from the reaction temperature and the sample machined from the capsule and crucible.

1.3.3 Kinetics of the Reaction between Boron Fibers and Mg Metal

1.3.3.1 Undoped Boron Fibers: The extent of reaction between boron fibers and magnesium metal was measured in situ using x-ray diffraction from synchrotron x-ray radiation. Synchrotron experiments were performed at the DuPont-Northwestern-Dow Collaborative Access Team (DND-CAT) Synchrotron Research Center at the Advanced Photon Source, Argonne National Laboratory. Figure 19 shows a diagram of the reaction chamber used for the in situ XRD measurements [34]. Unreacted samples were prepared by infiltrating boron fibers with magnesium in a titanium crucible. The boron fiber volume fraction was designed to be ~20% after infiltration which would produce an MgB₂ volume fraction of ~37% after reaction. The crucibles were thinned to a wall thickness of 250 μm to minimize absorption of the x-ray beam, and sealed with steel compression fittings before enclosure in a quartz vacuum chamber where the sample was balanced on a Type K thermocouple in the middle of an IR furnace. The furnace had two windows that allowed x-rays to pass through the quartz chamber wall and Ti crucible containing the Mg/B sample. The furnace was placed in the 5-BMD beamline at DND-CAT where a monochromatic 65 keV ($\lambda = 0.019$ nm) x-ray beam with 1 x 1 mm cross section passed through the sample and produced a 2-D diffraction pattern on a gain intensified charge-coupled device (CCD) camera (Photonic Science Limited, UK). The camera software was programmed to take an exposure every 30 s to 3 min after the sample reached the desired temperature. Using Fit2D software at DND-CAT, the 2-D image files were converted into plots of intensity vs. diffraction angle 2θ through integration of pixel intensities 360 degrees around the diffraction ring image and conversion of radial distance from the center of the ring into diffraction angle. The camera was positioned ~ 380 mm from the sample so that the $\langle 101 \rangle$ MgB₂ peak just fit onto the CCD screen. MgB₂ formation was measured using the normalized integrated intensity of the $\langle 101 \rangle$ MgB₂ diffraction peak. The $\langle 101 \rangle$ MgB₂ peak was monitored since it was the strongest peak for MgB₂ and did not overlap with other materials used in the experiment (i.e. Ti, Mg, quartz). A combination of custom Java codes was used to subtract a background file (a diffraction pattern during heat up or at $t = 0$ where the Mg is melted and Ti has started recrystallization). Jade 6.5 powder diffraction analysis software (available in the Cohen X-Ray Diffraction Facility at Northwestern University) measured the MgB₂ $\langle 101 \rangle$ peak area for each pattern. The resulting series of peak areas were then normalized using the sample after it had completely reacted to MgB₂ (determined by metallography) and plotted as a function of time. Figure 20 shows a summary of reaction times at temperature ranging from 885° to 1000°C. At temperatures of 925°C and above, the fiber was fully reacted to MgB₂ in under two

In situ reaction kinetics measurements

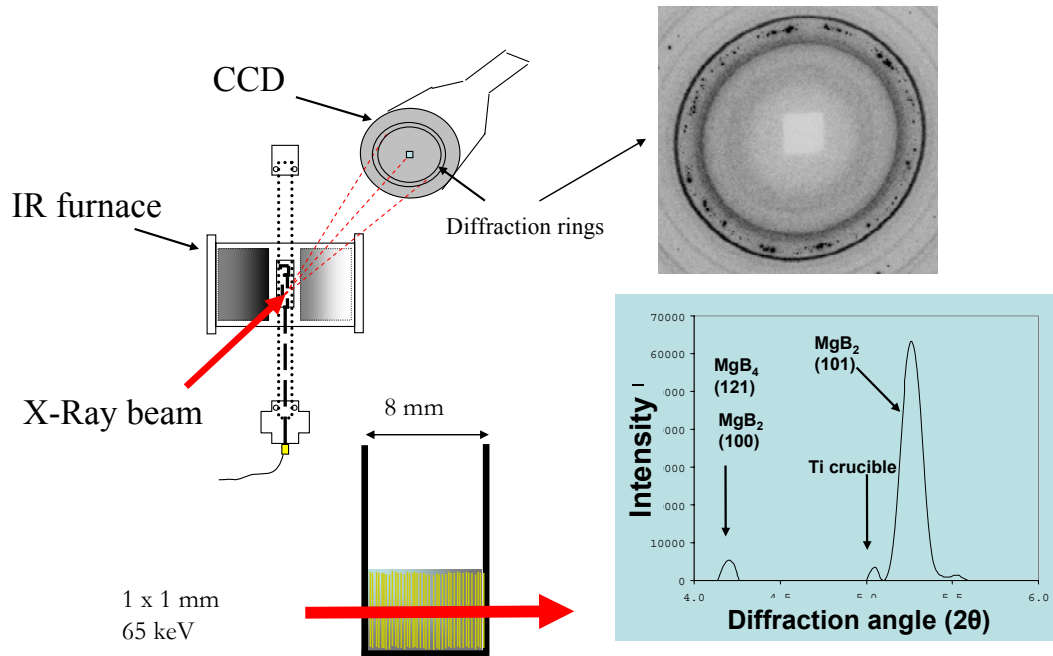


Figure 19. Experimental setup showing the reaction chamber used for in situ x-ray diffraction measurements [34]. MgB₂ formation was measured using the normalized integrated intensity of the 101 MgB₂ diffraction peak.

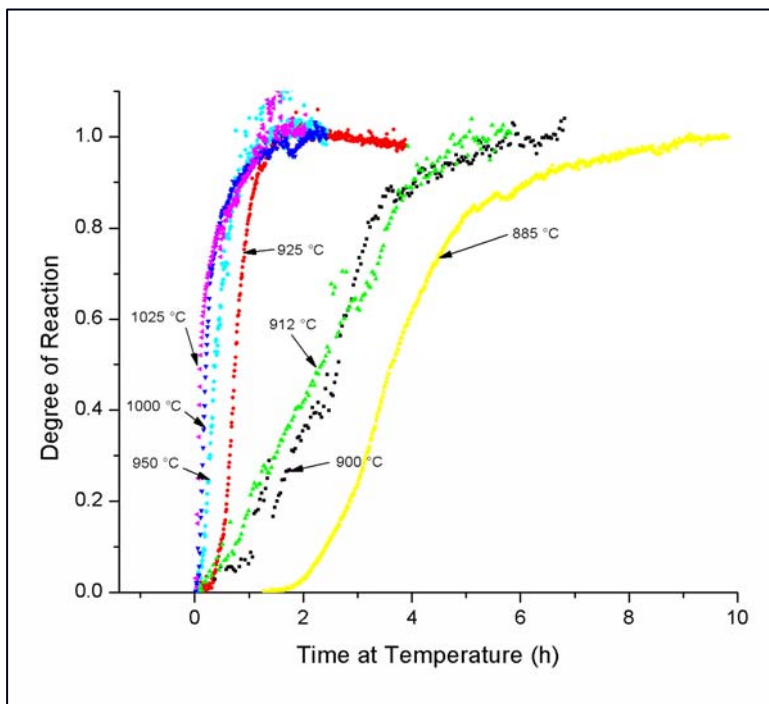


Figure 20. Plot tracking the reaction between Mg and undoped boron fibers at various temperatures

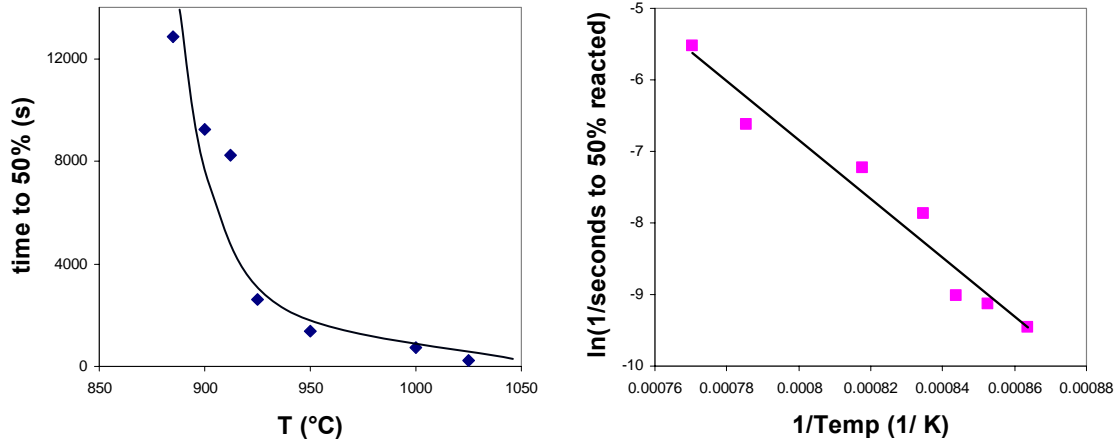


Figure 21. Reaction rate plots $\text{Mg} + \text{B}_{\text{fiber}} \rightarrow \text{MgB}_2$. The left plot shows the time to achieve 50% reaction vs temperature. The right plot shows that the reaction follows Arrhenius behavior.

In situ Mg/MgB₂ composites

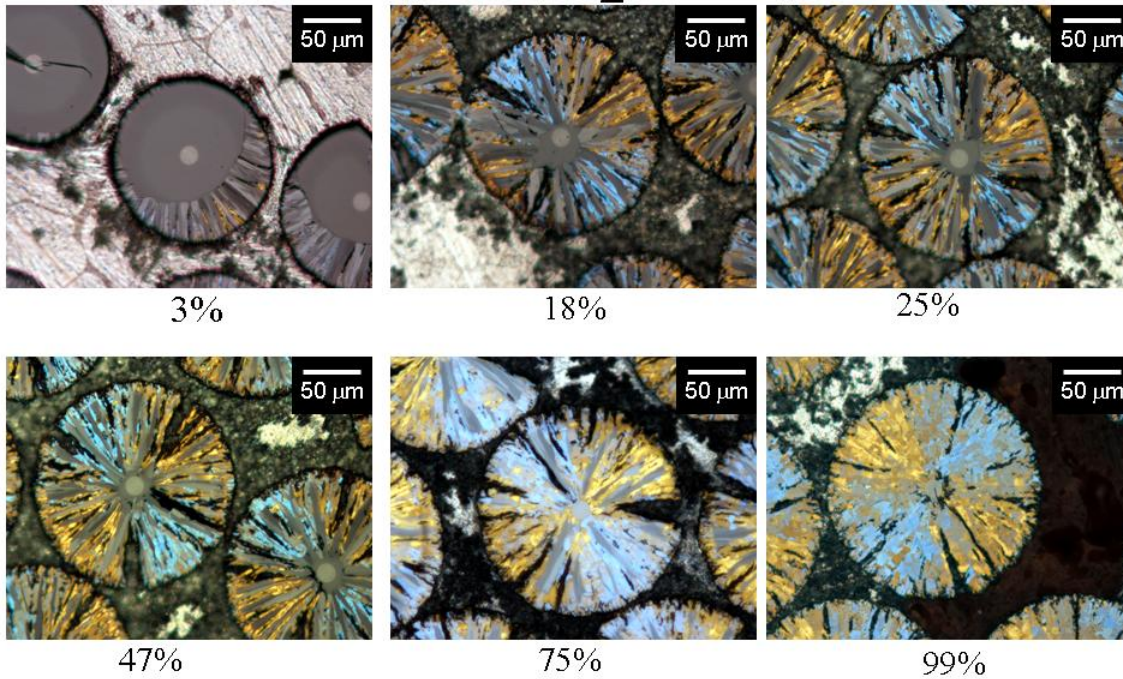
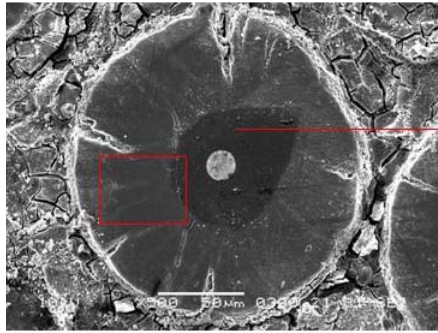
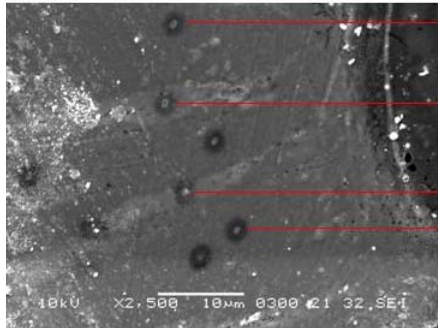


Figure 22. Polarized optical micrographs of Mg/MgB₂ composites showing cross sections of fibers that have reacted to MgB₂ at progressive stages of completion. Fibers are multiphase until the reaction is complete. Volume expansion accompanies the conversion of boron to MgB₂. This expansion causes radial cracks in the fiber which facilitates further infiltration of Mg metal into the fiber.



→ Unreacted boron



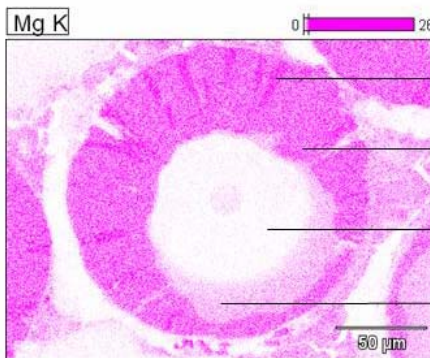
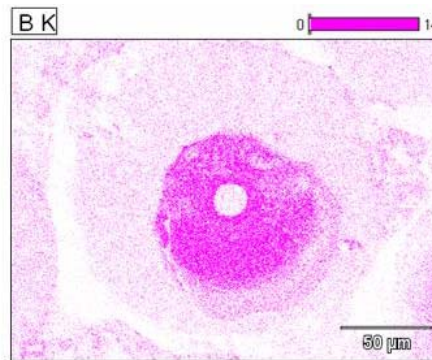
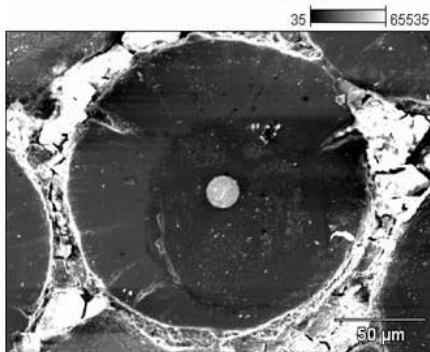
→ MgB₄

→ MgB₂

→ MgB₂

→ MgB₄

Figure 23. Fiber-Mg composite in which the boron fiber partially reacted with Mg. SEM micrographs indicate presence of at least three phases. The dark-colored center phase around the tungsten boride substrate is unreacted boron. The remainder of the fiber appears to consist of two phases. EDS spot analysis of the light-colored phase is consistent with MgB₂; spot analysis of the darker colored predominant phase is consistent with MgB₄.



→ MgB₂

→ MgB₄

→ B (unreacted)

→ MgB₇

Figure 24. Energy dispersive x-ray spectral (EDS) images of partially reacted fiber cross section showing unreacted boron, MgB₇, MgB₄, and MgB₂. Upper left photo is the SEM image, lower left is the Mg x-ray image, upper right is the boron x-ray image.

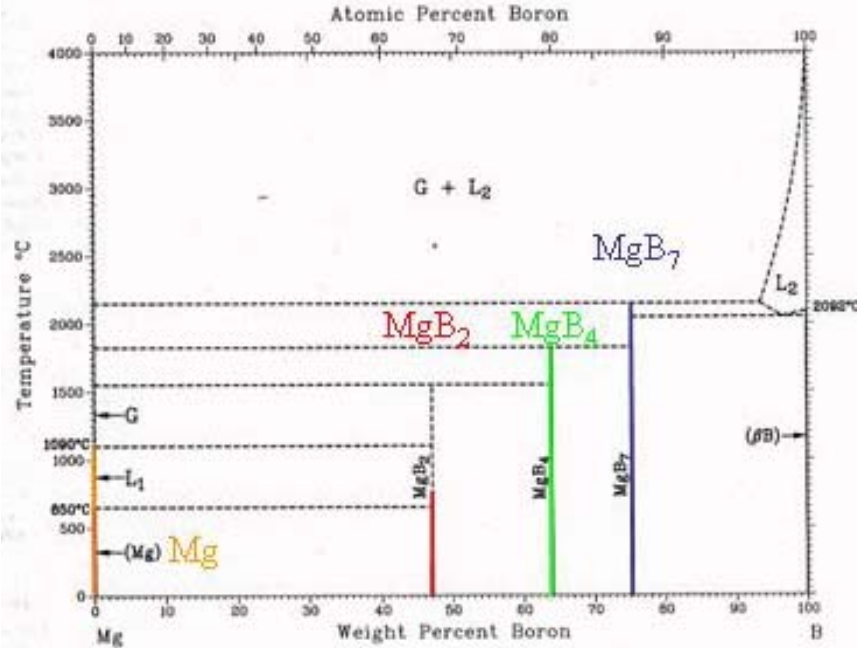


Figure 25.
Mg-B phase
diagram [38].

hours. As one would expect, the reaction time becomes progressively longer at lower temperatures. The reaction rate plot in Figure 21 indicates that the reaction rate has Arrhenius-type temperature dependence.

The reaction between boron fibers and magnesium metal in the liquid infiltrated fiber-metal composites was characterized by several methods. Figure 22 shows a series of reflected polarized optical micrographs of polished composite cross sections as the Mg + B reaction reached progressive stages of completion. Polarized optical microscopy showed that within a composite there were significant local variations in boride phase development from fiber to fiber as the reaction proceeded to completion. The micrographs also indicated the presence of multiple phases in the partially reacted fibers. Fibers are multiphase until the reaction is complete. Volume expansion accompanies the conversion of boron to MgB₂. This expansion causes radial cracks in the fiber which facilitates further infiltration of Mg metal into the fiber. Energy dispersive x-ray analysis in the scanning electron microscope (SEM/EDS) indicated that up to four phases may be present in the fiber during the course of the reaction. Figures 23 and 24 show the results of EDS analysis using both point analysis mode and spectral imaging. The analyses indicated the presence of unreacted boron, MgB₇, MgB₄, and MgB₂. The presence of multiple phases indicates, as expected, that equilibrium has not been achieved in partially reacted composites. The phases found by SEM/EDS analysis are consistent with those reported in the Mg-B phase diagram [38] shown in Figure 25.

1.3.3.2 Doped Boron Fibers: Doped boron fibers were also infiltrated with liquid Mg and then reacted further. In the case of the doped fibers the B + Mg reaction proceeded much more slowly by three orders of magnitude. Undoped boron fiber can typically be completely reacted to MgB₂ in 30 minutes at 1000°C, whereas the incorporation of even tenths of a percent of Ti or C dopant needed ~100 hrs for the reaction to go to 50% completion. Figure 26 is a polarized optical micrograph of a cross section fiber-metal composite in which the Ti-doped boron fiber

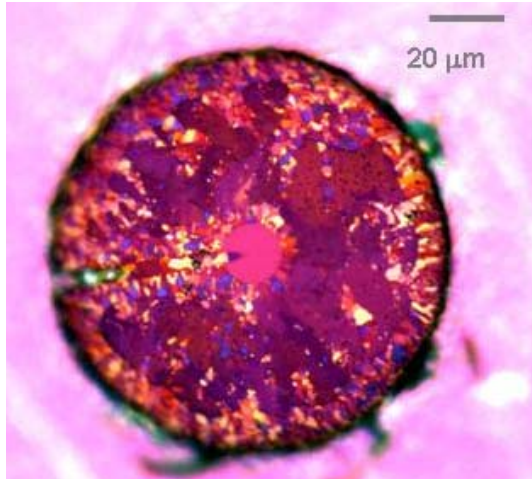
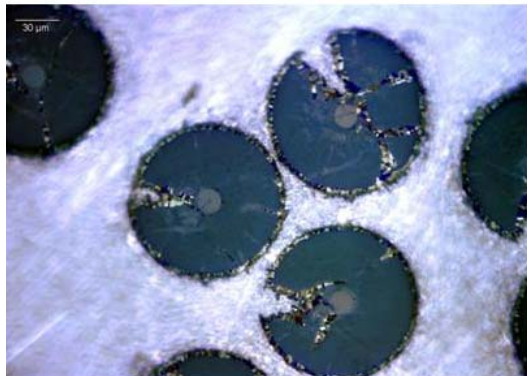


Figure 26. Ti-doped boron fiber
38% reacted with Mg (36 hr,
1000°C)

Mg infiltrated C-doped B fibers



Infiltrated at 800°C;
then 7°C/min to 1000°C and
held for 16.5 hrs followed by a
7°C/min cool

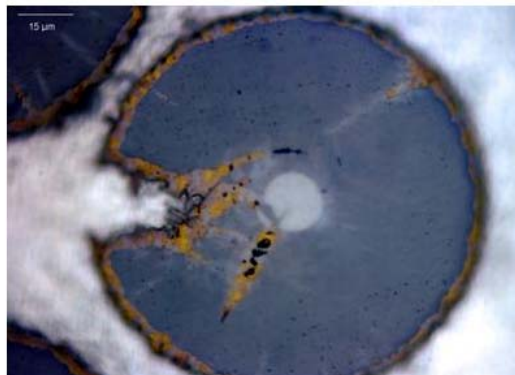
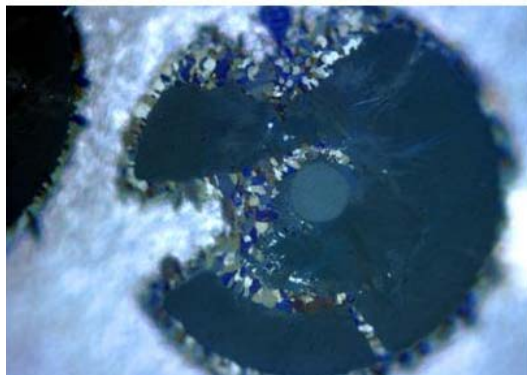


Figure 27. Doped boron fibers reacted with Mg in a metal matrix composite produced by liquid metal infiltration. After over 16 hr at 1000°C, only a small percentage of the fiber is converted to MgB_2 .

(Ti/Mg ratio = 0.6 atomic%) had reacted 38% to MgB_2 after a heat treatment at 1000°C for 36 hours. Figure 27 shows optical micrographs of fiber-metal composites in which the C-doped boron fiber (carbon concentration = 0.5 atomic%) had reacted to <5% completion after a heat treatment at 1000°C for 16 hr. In fact the 0.5% C-doped B fiber required 96 hr at 1000°C to achieve 50% reaction to MgB_2 .

1.3.4 Initial Studies to Identify the Reaction Mechanism

It was observed that incorporation of dopant impurities into B fibers even at low concentrations of <1 atomic% resulted in significant decreases in the reaction rates during the reaction to doped MgB_2 in the infiltrated fiber-metal composites produced in this Phase I project. This decrease in reaction rate is consistent with observations of the reaction rate of doped B fiber with Mg vapor [7] and motivated the work reported below, in which doped B fibers are characterized prior to and after their conversion to MgB_2 [35].

1.3.4.1 Characterization Equipment: SEM/EDS analyses were carried out on a digital SEM (JEOL 5610), and a ThermoNoran System Six EDS system. TEM analyses were performed on a JEOL 2010-FEG (field emission gun) microscope operating at 200kV and a Philips EM420 operating at 100kV. EDS analyses were carried out in STEM (scanning transmission electron microscopy) mode, using an EDAX EDAM-III detector with Emispec Cynapse software. X-ray diffraction patterns were obtained using a Scintag Model XDS-2000 x-ray diffractometer calibrated with a NIST silicon standard. Copper $K\alpha$ radiation was detected with a germanium crystal cooled to 77K. The diffraction patterns were taken in the range of $2^\circ \leq 2\theta \leq 70^\circ$ with a scan rate of $0.1^\circ 2\theta$ per minute.

1.3.4.2 Results: A series of SEM micrographs of boron fiber surfaces (Figure 28) shows fiber surface morphology as a function of carbon doping level. Undoped CVD B fibers appear amorphous by TEM. X-ray diffraction patterns (Figure 29a) are indicative of an amorphous phase. The “corn-cob” surface texture (insets to Figures 28a and 28b) is indicative of macroscopic growth morphology and not the size of individual grains. Below a carbon dopant level of 2%, the fiber surface morphology remained relatively unchanged and the boron phase remained x-ray amorphous. At the 2% dopant level, however (Figure 28c) there were isolated occurrences of much larger grains, 10-50 μm in size, that were most likely seeded by a threshold concentration of carbon dopant. At the 3% dopant level (Figure 28d) rapid crystal growth dominates and the fiber no longer retained a regular cylindrical shape, but rather was a string of larger 10-50 μm crystals irregularly arrayed around the tungsten boride substrate. X-ray diffraction of the 3% carbon-doped boron fiber indicates that it is well-crystallized tetragonal boron (Figure 29c). TEM was performed on fiber surfaces, broken shards of fibers, and samples prepared by ion beam thinning. High resolution TEM did not detect crystalline grains in the undoped B fibers. Tilting dark field imaging also did not exhibit significant crystallinity, indicating that the undoped B fibers are primarily amorphous, which is consistent with the above x-ray diffraction results. TEM observation of the crystallized fibers doped with 3% carbon showed grains >10-20 μm in size at the surface of the fiber. Selected area diffraction (SAD) showed that the fibers doped with high levels of carbon crystallized with the tetragonal phase of boron [36]. High resolution TEM images acquired at the [111] orientation were consistent with tetragonally crystallized boron formation in the 3% carbon- doped boron fiber. Quantitative

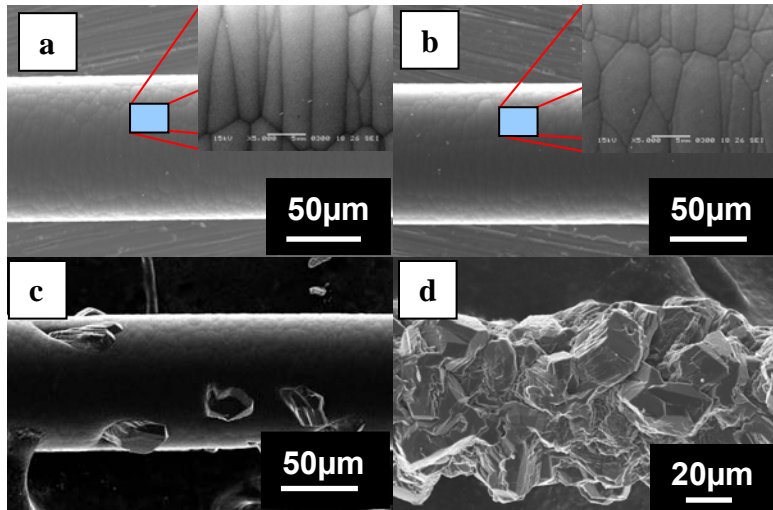


Figure 28. Surface morphology of boron fibers at the following carbon dopant levels in atomic percent: a) 0% b) 1.4% c) 2% and d) 3%. Insets to 2a and 2b show a 25µm wide area of the fiber surface.

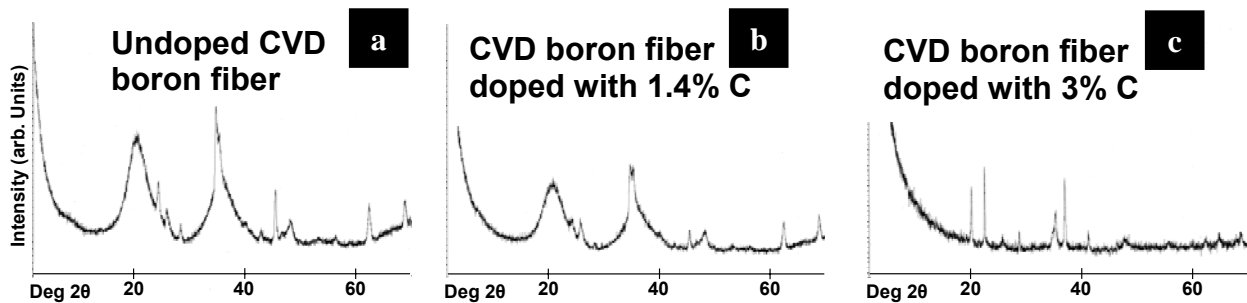


Figure 29. X-ray diffraction patterns of undoped and carbon-doped B fibers. Undoped boron and boron doped with 1.4% carbon consist of amorphous boron plus crystalline tungsten boride substrate material. Boron doped with 3% carbon is a well crystallized tetragonal boron phase.

EDS performed on spectra acquired from several thicknesses of crystallized B determined that carbon is present within the crystal and was not merely a surface contaminant during the analysis. Quantitative EDS also established that the carbon concentration is significantly less than 20 atomic %, thereby indicating the crystalline phase is not B_4C . Although over twenty B(low-C) phases are reported in the Powder Diffraction File (PDF) [37], the electron diffraction data of these crystallized fibers match best to results reported for pure tetragonal boron (PDF-74-0945). It is thus suggested that some of the many "pure" boron phases reported in the PDF may have some solubility for carbon.

TEM samples were prepared in cross section of the Mg-infiltrated B fibers, using polishing, dimpling and ion-beam thinning. The B fibers strongly resist thinning as compared to the surrounding matrix metal grains. Figure 30a is a bright field image of the interface between undoped B fiber and matrix in a composite infiltrated at 800°C. Four regions are visible: (i) the

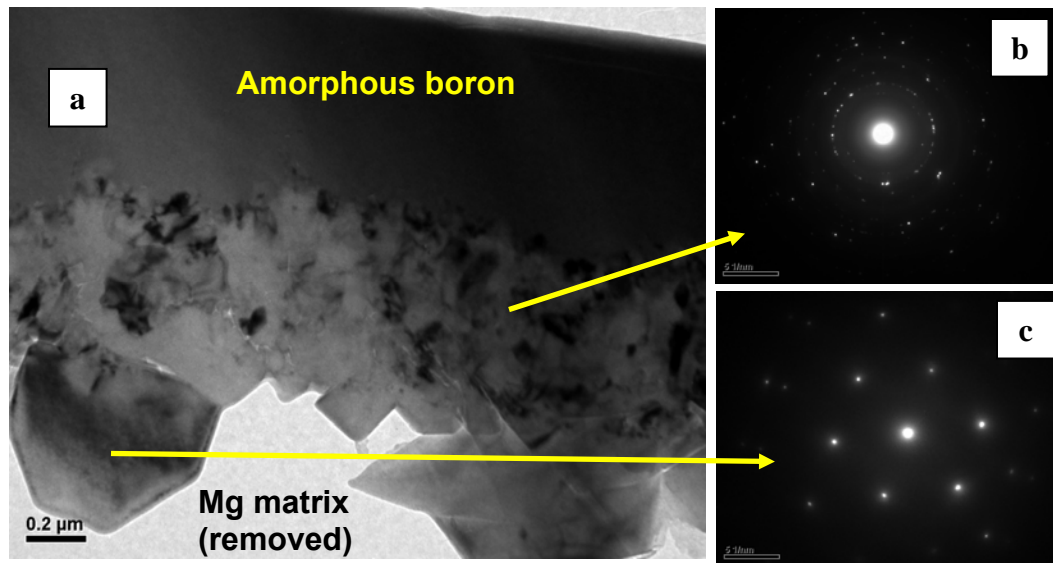
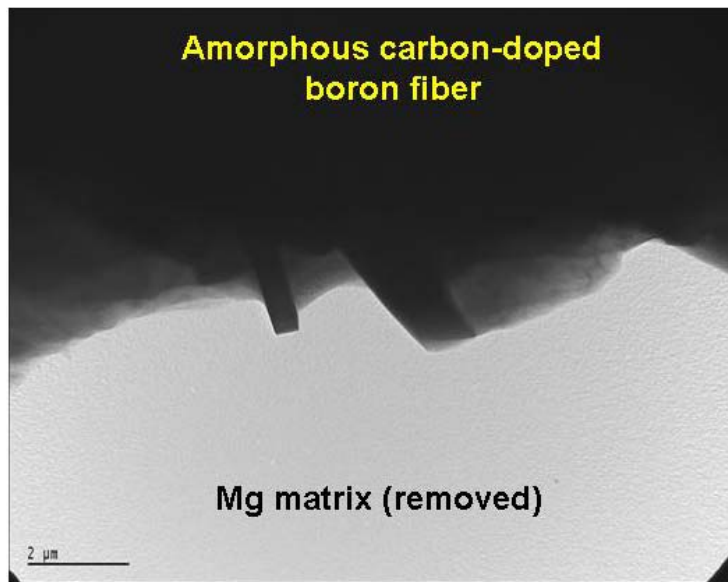
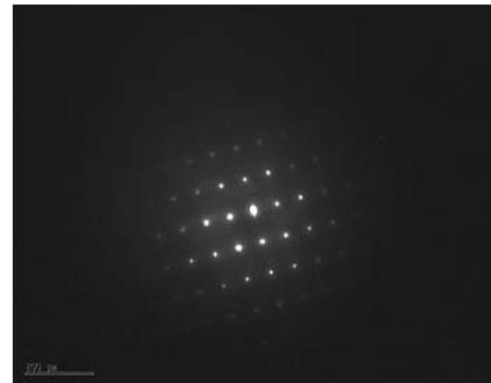


Figure 30. Bright-field TEM image (**30a**) at interface of undoped boron fiber and Mg matrix. **30b** shows SAD of the finer-grained phase (SAD ring pattern consistent with MgB_4 or MgB_{12}), and EDS was consistent with a phase that is more boron-rich than the MgB_2 phase. **30c** shows SAD indexed with the $[-1100]$ zone orientation of the MgB_2 hexagonal phase.

fiber interior (top region of 30a) is amorphous B; (ii) closer to the fiber-matrix interface is 0.5 μm zone of fine grains (20-50nm); (iii) the fiber surface consists of a 1-2 μm zone of coarser $\sim 1 \mu\text{m}$ grains; (iv) the bottom region in Figure 30a consists of the Mg matrix which was preferentially removed by TEM sample preparation. Figure 30b exhibits SAD of the fine-grain zone, with ring diffraction consistent with several B-Mg phases (such as MgB_4 or MgB_{12}). Figure 30c exhibits SAD of the next region with a $[-1100]$ zone axis of the MgB_2 hexagonal phase. TEM analysis of the Mg matrix showed Mg metal grains $>10\text{-}20 \mu\text{m}$ in size extending across the entire matrix region between fibers. As infiltrated at 800°C , the reaction between B and Mg was limited to two thin layers indicated in Figure 30. Figure 22 shows optical micrographs of cross sections of composites that were heat treated at 1000°C (after the initial 800°C infiltration). A significant fraction of the undoped boron fibers reacted with the Mg after 15 min at 1000°C . The 0.5% C-doped boron fibers (Figure 27) reacted much more slowly with the Mg matrix, exhibiting a reaction zone of $<5 \mu\text{m}$ after more than 16 hr at 1000°C . The presence of carbon apparently inhibits the reaction between B and Mg, although the reason for this is not clear. The undoped and 0.5% C-doped boron fibers are both amorphous with similar crystallite sizes. Carbide phases at the C-doped fiber-matrix interface were not observed by TEM examination (Figure 31), although partial material loss during sample preparation could explain this. SEM/EDS analysis of the partially reacted zones (Figures 23 and 24) indicated a boron-rich composition suggesting that MgB_4 and/or MgB_7 form prior to complete reaction of the fiber to form MgB_2 . This is consistent with previous reports [14] in which boron fibers were reacted with Mg vapor. TEM analysis of Mg-B composites that were annealed at 950°C for 1 hour after the initial infiltration showed evidence of MgB_2 formation in the Mg matrix $>100 \mu\text{m}$ from the fiber-matrix interface.



Bright field image of interface



Selected area diffraction (SAD) of grain at interface consistent with MgB_{12} or MgB_4

Figure 31. TEM of interface between carbon doped boron fiber and Mg metal in a fiber-metal composite made by liquid Mg infiltration. No carbides that might act as diffusion barriers were identified at the interface, but more work is needed.

The microstructure of boron fibers made by CVD was examined as a function of carbon dopant level. Undoped fibers and fibers doped with carbon at levels of <2 atomic % were found to be amorphous. At carbon dopant levels at $\geq 2\%$, the growth of large ($10\text{-}50\mu\text{m}$) grains of crystalline tetragonal boron was observed. It is suggested that there may be carbon present in the crystalline tetragonal phase of boron observed in fibers that were doped with higher concentrations ($\geq 2\%$) of carbon. Doped and undoped fibers were infiltrated with molten magnesium to form boron/magnesium metal matrix composites. At the 800°C infiltration temperature, a layer of MgB_2 was observed adjacent to the Mg matrix and a layer of boron-rich phase or phases (MgB_4 and/or higher borides) were observed adjacent to the boron fiber. Additional reaction at $950\text{-}1000^\circ\text{C}$ resulted in further conversion of the fibers into a mixture of MgB_2 and higher borides (e.g. MgB_4), as well as increased formation of MgB_2 further into the Mg matrix. It was observed that C-doped boron fibers reacted with Mg much more slowly than undoped B fibers. Additions of carbon lower than 1% had a significant rate on the rate of formation of MgB_2 . This was consistent with previous reports [7] on the rate of reaction between C-doped boron fiber and Mg vapor, but was still somewhat surprising. A hypothesis of the formation of a diffusion barrier at the interface between Mg and doped B fibers was not born out by observation. Carbides or other phases which perhaps would act as interfacial diffusion barriers were not observed at the fiber-matrix interface of the carbon-doped boron fibers reacted with Mg at $950\text{-}1000^\circ\text{C}$. More work is needed, however, to definitively characterize the interface between a doped boron fiber and the Mg metal matrix.

1.3.5 Superconducting Properties of MgB₂ made by Liquid Metal Infiltration

A carbon-doped composite made by liquid metal infiltration was reacted at 1000°C for 96 hours. It was estimated from polarized microscopy of metallographic cross sections that the fibers had reacted approximately 50% to MgB₂. The partially reacted fibers were leached from magnesium matrix with hydrochloric acid and the superconducting properties were measured. Figure 32 shows the J_c results derived from magnetization hysteresis loops. Results are nearly identical to those reported [7] for C-doped MgB₂ made by the reaction of doped B fibers with Mg vapor.

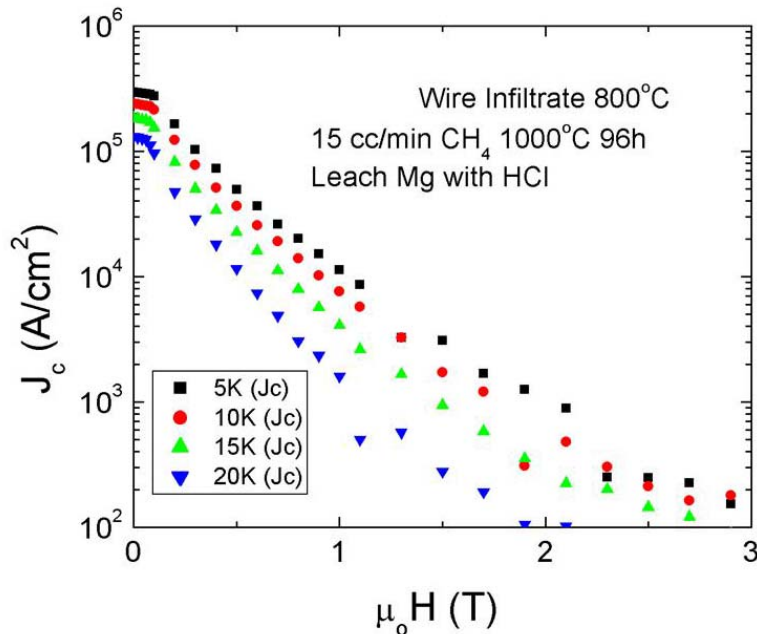


Figure 32. Critical current densities of 0.5% C-doped fibers from a fiber-metal composite made by liquid infiltration and subsequently reacted at 1000°C for 96hr.

1.3.6 Plasma Synthesis of Doped Boron Nano-Sized Powder

In order to provide an alternate source of boron as a raw material for the fabrication of high critical field MgB₂ wires, the plasma synthesis of boron nanopowder was investigated. The results of these efforts were largely described in section 1.1.7. Because of the small particle size and large surface area of the powder, the rate of the reaction between Mg and doped boron fiber was orders of magnitude faster than that between Mg and B fiber. As reported in section 1.1.7, the superconducting properties (J_c and H_{c2}) of the MgB₂ superconductors made from the plasma synthesized boron nanopowders are among the highest reported to date for bulk MgB₂.

1.3.7 Liquid Metal Infiltration of Plasma Synthesized Doped Boron Nano-Sized Powder

Doped and undoped plasma synthesized boron nanopowder were infiltrated with liquid Mg to form powder-metal composites. An example of an infiltrated sample is shown in Fig. 33.

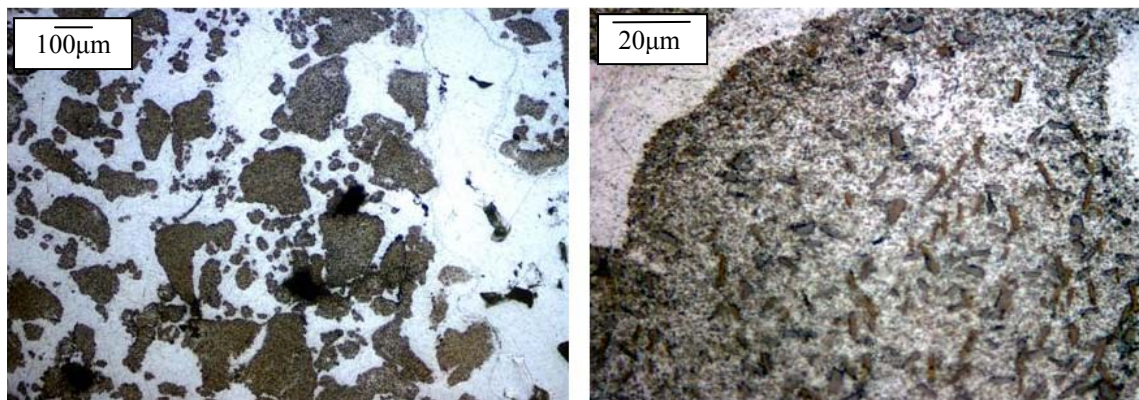


Figure 33. Optical micrograph of a polished cross section showing plasma synthesized boron powder infiltrated with liquid magnesium. In this initial experiment, infiltration took place both on a macro scale around $\sim 100\mu\text{m}$ agglomerates and on a smaller scale around $<1\mu\text{m}$ particles and agglomerates.

In these initial experiments infiltration took place both on a macro scale around $\sim 100\mu\text{m}$ agglomerates and on a smaller scale around $<1\mu\text{m}$ particles and agglomerates. After the infiltration at 800°C , the composites were reacted at 1000°C for 1 hr. Three reacted composites were analyzed by x-ray diffraction. Composite sample P427 used undoped boron powder; sample P426 used boron powder co-doped with 2% Ti and 1.6% C; sample P429 used boron powder co-doped with 0.6% Ti and 1.2% C. The x-ray diffraction patterns in Figure 34 show that in all cases the reaction to MgB_2 went to completion.

All three composites were machined into parallelepipeds in order to measure the superconducting properties. These are shown in Figure 35. The left-hand plot of Figure 35 shows magnetization as a function of temperature. As expected the presence of dopants results in a decrease in T_c . The right-hand plot of Figure 35 shows the critical current density, J_c , as a function of magnetic field strength. Since the volume fraction of boron in the metal-powder composites is $<40\%$ it was expected that J_c would be because of weak-link behavior due to the presence of excess Mg. The observation of superconductivity in these powder metal composites is however quite encouraging. J_c should increase as the volume fraction of the boron powder increases.

1.3.8 Fabrication of Wire by PIT using Doped Boron Nano-Sized Powder

The properties of plasma synthesized boron powder were further evaluated by their fabrication into superconducting wires by the powder-in-tube method. A cross section of a PIT wire was shown in Figure 17, Section 1.1.8. Figure 36 shows J_c (measured from magnetization hysteresis loops) as a function of magnetic field strength for PIT wires reacted at 700°C for various times. In all cases, the C-doped boron nanopowder reacted to MgB_2 to near completion. The PIT wires could be reacted in times on the order of 10 minutes and still exhibit J_c greater than 10^5 A cm^{-2} at 5K and 2T.

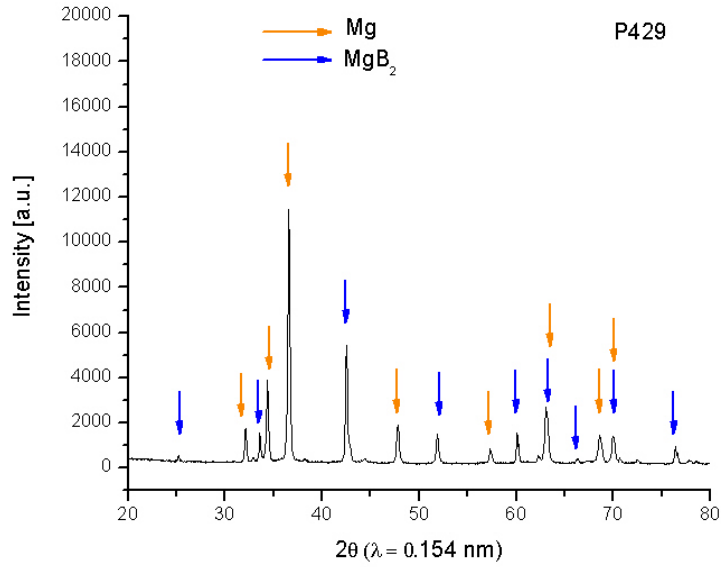


Figure 34. X-ray diffraction patterns of boron nanopowders infiltrated with liquid Mg and then further reacted for 1 hr at 1000°C. The reaction to MgB₂ went to completion when undoped boron powder was used (P427) or the powder was doped with Ti and C (P426, P428).

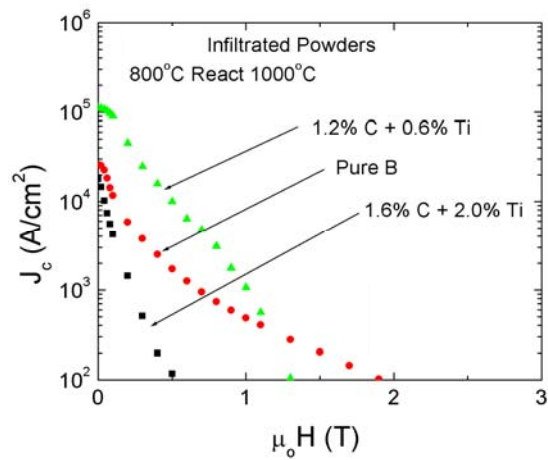
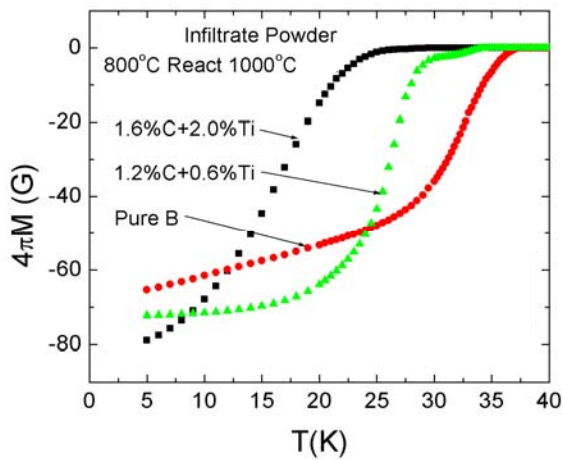
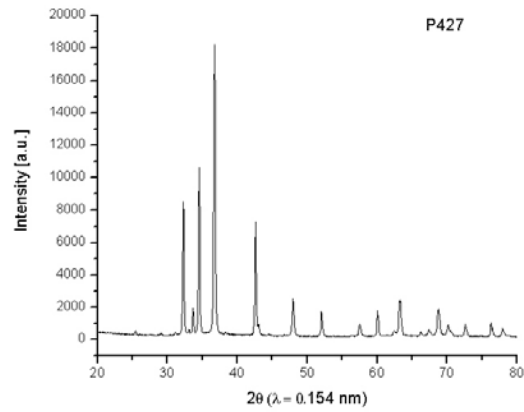
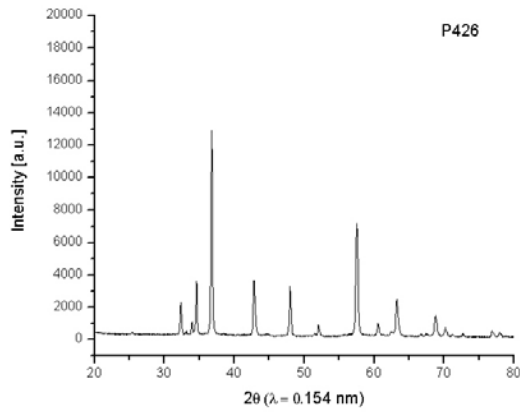


Figure 35. Superconducting properties of composites made by the infiltration of doped and undoped boron nanopowder.

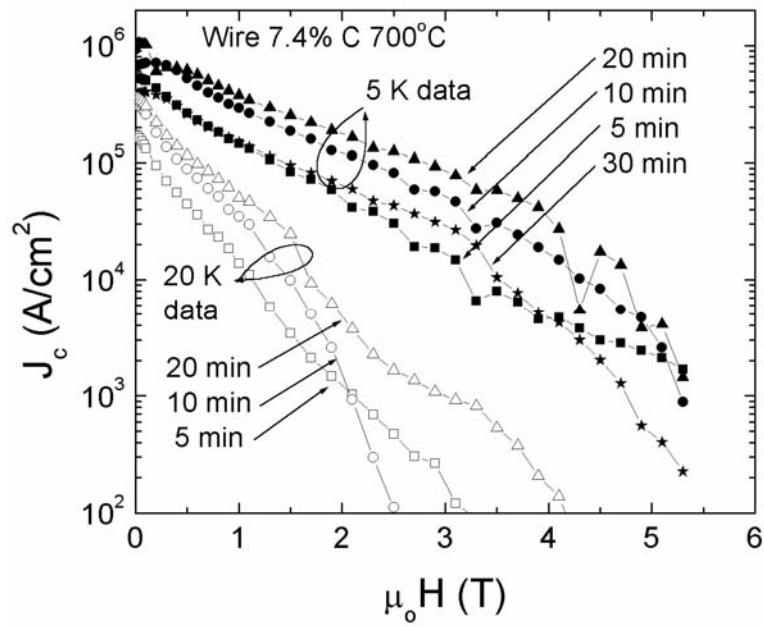


Figure 36. Comparison of J_c data for PIT wires made from plasma synthesized doped boron nanopowder. Very nearly full reaction occurs for wires heated at 700°C for a range of times.

2.0 Suggested Further Work

2.1 Technical Objectives of Further Work:

The technical objectives section is written in a format that states the problem and proposed solution.

- **Problem:** The critical current densities, J_c , and upper critical fields, H_{c2} , of undoped MgB_2 are not high enough for a commercial superconducting wire, independent of whether the MgB_2 is formed by Mg vapor reacting with B fiber, by infiltration of B fibers to form composites of MgB_2/Mg , or by hot pressing of MgB_2 powder to a desired shape.
- **Proposed Solution:** Continue to dope the boron fiber by CVD methods to achieve very fine-scale dispersion that result in the enhancement of J_c and H_{c2} . To date, Ti doping raises J_c , presumably by adding precipitates that enhance magnetic flux pinning [5,6]. C-doping raises H_{c2} , presumably by a perturbation of the crystal structure resulting in a shorter electron mean free path [7]. Continue fine-scale doping dispersion in plasma synthesized nano-scale powder by direct injection of dopant precursor gases into the plasma.

- **Problem:** The rate of reaction between Mg and doped boron fibers is very slow. The long reaction times result in grain growth, which coarsen dopant precipitates and decrease J_c .
- **Proposed Solution:** Continue investigations to identify the mechanism which significantly slows the kinetics of the reaction. Initial cross-sectional TEM of the fiber-Mg interface was begun in Phase I, but more work is needed. Once a mechanism is identified, the best approach can be chosen from among the following:
 - Make alloy additions to Mg that increase the reaction rate.
 - Choose dopant impurities that will enhance J_c and H_{c2} , but not adversely affect kinetics of the Mg + B reaction.
 - Pursue the alternate path of using plasma synthesized nano-sized doped boron powder, which will radically shorten the diffusion path of Mg and increase the reaction rate. It has recently been demonstrated that Specialty Materials powder can be homogeneously doped and has produced superconductors with high values of J_c ($>10^5$ A cm⁻² at 5-6 tesla and $H_{c2}(0) = 37$ tesla, **the highest reported to date** for bulk MgB_2 .) [8]

- **Problem:** The liquid infiltration process is currently carried out in batch mode, which is not practical for a commercial wire manufacturing process.
- **Proposed Solution:** Build a prototype apparatus that provides for continuous infiltration and long lengths of composite wire.

- **Problem:** Liquid infiltration of nano-sized boron powder with Mg may not provide sufficient continuous conduction path through the superconducting phase, thus resulting in weak link behavior and poor superconducting properties.
- **Proposed solution:** Pursue the alternate path involving powder-in-tube (PIT) wire processing using the nano-sized boron powder. This approach using Specialty Materials plasma synthesized powder has already produced very promising superconducting properties ($J_c = >10^5 \text{ A cm}^{-2}$ at 5-6 tesla, and $H_{c2}(T=0) = 37 \text{ tesla}$) [ref]. A drawback to the PIT method is the presence of porosity in the MgB_2 phase because of the net negative volume change when stoichiometric quantities of Mg and B are reacted in a confined volume. The ultimate goal is to optimize a wire production method that minimizes the drawbacks of PIT (porosity) and liquid metal infiltration (weak link behavior, excess Mg).

2.2 Suggested Commercialization Plan

2.2.1 Company Information

Specialty Materials' mission is to consistently supply the highest quality boron and silicon carbide based products that help our customers solve problems and develop improved products. Our unique products provide enabling solutions for problems in a number of areas including structural integrity, controlled thermal expansion and engineered surfaces. Our core competence is gas phase processing, with specific expertise in chemical vapor deposition. Our core business at present is manufacturing Boron and SCS silicon carbide fibers and preforms. Materials are manufactured to aerospace tolerances through tight process control with complete traceability from our quality records all the way back to our starting raw materials, and we have achieved ISO 9001 certification.

Our strategic vision is to concentrate on these core strengths, and rely upon others to provide services that complement our expertise. We expect to grow the company organically, rather than through acquisitions. In the words of at least one corporate strategic planning guru, we "stick to the knitting", and do not venture far away from those things that we do well. Our base business is selling boron/epoxy tape preforms to aerospace, sporting goods, and industrial users who convert that to a composite material to solve challenging structural problems. Emerging markets include expanding that product line to controlled thermal expansion space structures applications, graphite and boron fiber hybrids, and new sporting goods applications. SMI is also increasing the silicon carbide fiber business for high temperature metal matrix composites and an industrial application for photovoltaic cells. Specifically, boron fiber and boron/epoxy tape preforms represent 60% of our business, with silicon carbide fiber products accounting for an additional 35% of our ~\$7M annual sales. This is accomplished with 36 full-time employees.

One can get a better sense of our market by putting it in the context of the market for other fibers. The worldwide supply of fiberglass is roughly 4B lbs., and it sells for ~\$1/lb. This translates to an annual market of ~\$4B with many customers. The annual volume of graphite fiber sold worldwide is approximately 40-50M lbs., with a typical selling price of \$15-30/lb, or roughly a \$1B annual market. Again, there are many customers for this product. Conversely, boron fiber sales worldwide are about \$6M from ~7,000 lbs sold at ~\$900/lb. Our silicon carbide fiber is more expensive still at an average selling price of \$3700/lb. Because of our extremely unique products (we are the only manufacturer of boron fibers in the world) and relatively high costs, there are fewer potential customers than for other fiber materials. To succeed in the marketplace, we attempt to drive potential customers to our website, and ultimately to us through technical presentations and publications, advertising, and promotion of our products at trade shows. While we do use sales personnel and call upon our customers regularly, having an extensive sales force that covers several geographical areas would not be productive from the perspective of cost versus expected results.

In fact, several of our most recent applications have resulted from prospective customers coming to us for the potential solution of a problem. These include controlled thermal expansion space structures using our boron fiber, photovoltaic cell manufacturing using our SCS silicon carbide fiber, and the development of boron-coated graphite parts for potential use in the semiconductor processing industry. The first two applications have resulted in viable new businesses, while the last one is under development.

Our development efforts in MgB₂ superconductivity began shortly after Akimitsu's discovery of its superconductivity in 2001. We immediately began an IRAD (internal research and development) project to study the feasibility of chemical vapor deposition of MgB₂. Shortly thereafter, we began collaborating with Ames Laboratory, who successfully converted our boron fiber to MgB₂ and confirmed its superconductivity characteristics.

Both the boron-coated graphite and the MgB₂ applications have similarities, in that they are non-structural and both rely upon outside help to be successful. In the former case, we have employed external consultants to help us address critical technical issues, identify the right customers and provide them the right solutions. In the latter case, much like our Phase I DOE STTR, we are working with a wide range of organizations that have expertise that is quite different from ours, and which suitably complements our own expertise.

These two opportunities are completely consistent with our vision of where we expect to be within the next five years. We will continue to grow our core business of Boron and SCS silicon carbide fibers for structural applications. We will achieve additional growth by expanding our core strength of chemical vapor deposition and using our manufacturing infrastructure for additional products that solve our customers' specific problems. We will employ the use of consultants and strategic partners to complement our capabilities and provide a complete solution to the customer. When and if we are constrained by financial commitments, we will license the technology to others who can ultimately deliver the product to the customer.

Because SMI has had a relatively short life as a small business (SMI was formed in Dec 2001 when Textron Systems sold the assets to a private investor), we have had few government-funded programs. In fact, the only government-funded program at SMI to date has been the Phase I DOE STTR for which we are seeking this follow-on Phase II program. However, it should be noted that all of the key personnel from Textron continued in their former positions. From a business perspective, this allowed a seamless transition for all of our long-term customers.

Moreover, in its former life as a division of Textron, the organization had extensive experience with successfully bringing products to market that were developed through external funding. Our primary business lines of boron and silicon carbide fibers were developed through assistance from the Air Force. SMI continues the trend of more than 25 years of uninterrupted supply of boron/epoxy prepreg to Boeing for the F-15 aircraft and to Northrop Grumman for the F-14 aircraft. Our advanced boron and silicon carbide fibers and composites are used in a range of aircraft, space, sporting goods, and industrial applications, so we are familiar with a broad range of products, applications, and customers. Our most recent example of developing a new market for an existing product is the use of silicon carbide fiber in a commercial photovoltaic application. Furthermore, we have experience with regulatory agencies. In addition to successfully achieving ISO certification and passing subsequent audits, we have dealt with OSHA (Occupational Safety & Health Act) regulators, plus various state and municipality regulators while completing a plant expansion.

2.2.2 Market

The most current forecast for the worldwide market for superconductors (Table 4) was published in June 2002 (and updated in December 2004) by Conectus (**C**onsortium of **E**uropean **C**ompanies determined **T**o Use **S**uperconductivity), (<http://www.conectus.org>). This forecast is more conservative than one put forth by the Council of Superconductivity for American Competitiveness in 1998 (Table 4). Both these organizations make up the European and

American sections respectively of ISIS (International Superconductor Industry Summit). The tempering of the numbers from the earlier forecast is most likely due to a realization that HTS materials will have a more difficult path to commercialization than originally anticipated because of technical and economic issues mentioned earlier. Nevertheless, even the more conservative Conectus forecast still predicts a substantial and growing market. While actual figures from the Conectus forecast were in € (Euros), we have converted them to U.S. dollars since the exchange rate was roughly equal at the time of the forecast. These figures represent annual sales of materials, components, and sub-systems for superconductivity.

Both forecasts state that MRI as a medical diagnostic tool is still the largest current market for superconducting magnets, and that significant growth rates are expected to continue for this business. Emerging new businesses are defined as electric power, industrial processing, transportation, new medical applications, plus information and communication technologies. In addition to the general forecast listed in Table 5, Conectus developed a series of qualitative forecasts for the various specific applications comprising the total market for superconductors. For those markets which are not yet developed, Conectus broke down the timing for each of these applications into pre-commercial markets related to research activities, emerging markets, and established markets. These are shown in Table 6. While Conectus has broken down the applications into LTS and HTS applications, the high critical current density and upper critical magnetic field possible with doped MgB₂ allows it to be used in many of these applications.

Table 4 – World Markets for Superconductors (\$M)
 (Source: Conectus, December, 2001 <http://www.conectus.org>)
 (Revised, December, 2004)

YEAR	1997	2000	2003	2004	2010
Business Field					
Research & Technological Development (RTD)	355	415	550	500	680
Magnetic Resonance Imaging (MRI)	1400	1900	2100	2500	3850
Total of RTD & MRI	1755	2315	2650	3000	4530
New Large Scale Applications	35	25	55	30	410
New Electronics Applications	20	30	75	55	260
Total of Emerging New Businesses	55	55	130	85	670
TOTAL WORLDWIDE MARKET	1810	2370	2780	3085	5200
Market Shares for LTS				3050	4690
Market Shares for HTS				35	510

Table 5 – World Markets for Superconductors (\$M)

(Source: Council of Superconductivity for American Competitiveness, 1998)

YEAR	2004	2005	2006	2007	2008	2009	2010
MRI/NMR	5554	6440	7486	8723	10191	11719	13476
High Energy Physics	3688	3817	3950	4089	4232	4358	4488
<u>Power Utility Applications</u>							
Transformers		8	85	427	654	889	1814
Motors				20	41	106	215
Generators				4	10	44	60
Fault Current Limiters		6	19	47	111	252	309
SMES*			6	11	29	88	96
Total Utility Products		14	110	509	845	1379	2494

*Superconducting Magnetic Energy Storage

Clearly, the dominant market at present and in the near term for MgB₂ superconductors is MRI magnets, an application for which MgB₂ is well suited. These devices are now used routinely in nearly all moderate to large sized hospitals, with estimates of greater than 20,000 systems currently in use. Even small local hospitals employ the use of MRIs which can be loaded onto a truck bed and moved from one site to another, thus spreading the cost of the units among many users. Another growing trend is the increased use of open field MRI units which employ the use of smaller split coils, unlike the larger solenoid coils used in conventional closed MRIs. The advantages of the open field units include expanding the customer base to claustrophobic and large patients, and allowing real time diagnostics during a surgical procedure. Because of these trends, it was estimated at ISIS-13 (Jacksonville, FL, October 2004) that the market for MRI units will grow 8-10% annually.

The ultimate end customers for MRI superconductor magnets from SMI's perspective are MRI manufacturers. GE Medical Systems is the largest, with others including Phillips, Marconi, Siemens, Hitachi, and Toshiba. These MRI manufacturers typically purchase their magnet systems from suppliers such as Intermagnetics, Bruker, Oxford Instruments, and Ansaldo Superconductor. Superconductor magnet suppliers purchase cable from component suppliers such as NKT Cable, Pirelli, Sumitomo, and Furakawa.

Near term but yet to be developed markets include power utility applications such as transformers, motors, generators, fault current limiters, and other utility products. Major end users for such markets include GE Power Systems, Alston, Siemens, and Mitsubishi for power utility generators; General Dynamics and Rockwell for ship motors; Siemens ABB and General Atomics for transformers; and General Atomics for fault current limiters.

Table 6 – Estimated Milestones for Various Superconductor Applications

- ➡ pre-commercial orders related to RTD activities, field tests and prototype operation
- ➡ emerging market
- ➡ established market

LTS Large Scale Applications <i>Conectus, March 2004</i>					
Application	2003	2004	2005	2009	2013
Magnets for RTD	➡ ➡	➡ ➡	➡ ➡	➡ ➡	➡ ➡
Magnets for MR	➡ ➡	➡ ➡	➡ ➡	➡ ➡	➡ ➡
Cavities for Accelerators	➡ ➡	➡ ➡	➡ ➡	➡ ➡	➡ ➡
Magnets for SMES	➡ ➡	➡ ➡	➡ ➡	➡ ➡	➡ ➡
Magnets for Magnetic Separation	➡ ➡	➡ ➡	➡ ➡	➡ ➡	➡ ➡
Magnets for New Industrial Processing	➡ ➡	➡ ➡	➡ ➡	➡ ➡	➡ ➡
Magnets for New Medical Applications	➡ ➡	➡ ➡	➡ ➡	➡ ➡	➡ ➡

HTS Large Scale Applications <i>Conectus, March 2004</i>					
Application	2003	2004	2005	2009	2013
Current Leads	➡ ➡	➡ ➡	➡ ➡	➡ ➡	➡ ➡
Motors / Generators		➡ ➡	➡ ➡	➡ ➡	➡ ➡
Current Limiters		➡ ➡	➡ ➡	➡ ➡	➡ ➡
Power Cables	➡ ➡	➡ ➡	➡ ➡	➡ ➡	➡ ➡
Magnetic Bearings & Levitation		➡ ➡	➡ ➡	➡ ➡	➡ ➡
Insert Coils for High Field NMR			➡ ➡	➡ ➡	➡ ➡
Magnets for Industrial Processing			➡ ➡	➡ ➡	➡ ➡
Magnets for SMES			➡ ➡	➡ ➡	➡ ➡
Transformers			➡ ➡	➡ ➡	➡ ➡
Magnets for MR				➡ ➡	➡ ➡

LTS Electronics Applications <i>Conectus, March 2004</i>										
Application	2003		2004		2006		2009		2013	
SQUIDs for RTD	➔	➔	➔	➔	➔	➔	➔	➔	➔	➔
Mixers & Other Sensors for RTD	➔	➔	➔	➔	➔	➔	➔	➔	➔	➔
Voltage Standards for RTD	➔	➔	➔	➔	➔	➔	➔	➔	➔	➔
Magnetocardiography	➔	➔	➔	➔	➔	➔	➔	➔	➔	➔
Magnetoencephalography	➔	➔	➔	➔	➔	➔	➔	➔	➔	➔
Digital Circuits	➔	➔	➔	➔	➔	➔	➔	➔	➔	➔
Microprocessors										

HTS Electronics Applications <i>Conectus, March 2004</i>										
Application	2003		2004		2006		2009		2013	
Filters for Wideband Communication	➔	➔	➔	➔	➔	➔	➔	➔	➔	➔
Other Microwave Devices & Sensors	➔	➔	➔	➔	➔	➔	➔	➔	➔	➔
SQUIDs for Nondestructive Testing	➔	➔	➔	➔	➔	➔	➔	➔	➔	➔
SQUIDs for RTD	➔	➔	➔	➔	➔	➔	➔	➔	➔	➔
Magnetocardiography			➔	➔	➔	➔	➔	➔	➔	➔
Digital Circuits									➔	➔

Forecasts like those by Conectus and the Council of Superconductivity for American Competitiveness are based on complete systems and MgB₂ wire would be only a fraction of the overall market value. Based upon discussions with Mike Tomsic of Hyper Tech Industries, a fabricator of superconductor wires, we have made the assumption that wire represents 10% of a typical system. Thus, using the more conservative Conectus market figure of \$5200M for all superconductor applications in 2010, it could be said that the total potential market for MgB₂ wire is \$520 M in that year.

As stated in an earlier section, estimating magnitude and timing of projected sales for a product that does not yet exist always requires some assumptions. In our case, we have relied upon the business plan of Hyper Tech Research. They assume a \$70M business in MgB₂ for MRI units by 2009. This translates to roughly 40,000 lbs. of boron powder. Assuming a selling price of \$400/lb. for the boron powder, one arrives at a doped boron powder sales volume for MRI units in 2009 of \$16M.

We have made an assumption that we could achieve half of that boron powder market, or \$8M annually by 2009 for the following reasons. First, there are a limited number of boron powder suppliers, and virtually none of them to date have been able to supply high purity, doped

boron powder with the superconducting properties of ours. Moreover, we have patent protection for our technology that limits the ability of others to match our technology. Finally, we have a plant infrastructure in place, including an expensive gas recovery system that acts as a barrier to entry to others who might enter the marketplace. Assuming annual growth of 10% per year, we could envision sales of nearly \$15M in five years (2014). While many variables could affect these numbers either way, this indicates that a viable business could be achieved in less than five years. Further, it suggests that actual sales could be substantial by the end of this STTR program.

Clearly, \$8M in added revenue would be a huge benefit to Specialty Materials, Inc., yet at the same time, would be a sales volume we could comfortably achieve. If successful with this technology, not only will Specialty Materials be able to grow through expansion into a new market, it will also be able to utilize its existing capital equipment more efficiently, thus lowering its cost structure and adding more jobs.

DOE funding through the STTR program will accelerate our ability to develop both the doped fiber and doped powder approaches. It is estimated that even with Sumitomo's likely entrance into the marketplace with HTS wire by the end of this year, it is unlikely that there will be any MRI units employing materials other than conventional LTS materials before 2006. Best estimates for YBCO are closer to 2008, assuming the many technical problems are solved. We believe that with proper funding, our demonstrated technical successes to date, our ability to make product in volume, and our use of strategic alliances, we could have doped MgB₂ wire in a working MRI unit before any YBCO materials. Given a lead like that, the already strong economic advantages over YBCO materials would be extended by the possibility of volume business.

In order to achieve these potential sales volumes for MgB₂ superconductors and realize commercial success, SMI has developed an initial strategic plan. Specialty Materials will identify at least two high-probability superconducting applications for MgB₂ wire. The applications will be down-selected from work done during the STTR in which Specialty Materials evaluates up to four markets for MgB₂ wire and works with strategic partners in each of these markets. Any specific product development programs needed to commercialize the technology will also be identified in this effort.

The planning activity will be divided into two phases. In the first phase, we will review existing superconducting applications and confirm wire performance requirements and constraints in each application. We will then select two applications where MgB₂ could significantly improve cost and performance for existing products or planned future products. Current target applications are MRI systems and transformers.

We will utilize our strategic partners to implement this strategy. Should the doped powder approach be the best route, we would supply the boron powder to Hyper Tech Research, who would convert it to doped MgB₂. They, in turn, would supply MgB₂ wire to superconducting magnet manufacturers, who would supply it to MRI manufacturers. Conversely, if the doped fiber approach proves to be more promising, we would partner with a continuous caster like 3M who could make MgB₂ wire.

In addition to supplying materials to key players for evaluation, we will develop a comprehensive business plan. The business plan will: document the immediate customer's needs as well as the performance and economic benefits that would be realized in the end product; provide an analysis of competitive products and technologies; and determine how strongly the customers and end-users would be motivated to incorporate MgB₂ wire into their product. This

effort will include performance evaluations of MgB₂ wire. It will also outline MgB₂ wire product requirements for the market application, identify any additional application-specific experiments required, and define any product development programs needed for successful implementation. At the conclusion of the STTR program, SMI will publish the results of its efforts in technical and business trade journals; it will also present papers at the appropriate technical conferences. Where suitable business potential exists, it will work with strategic partners to develop and take to market specific products identified in the commercialization plan.

2.2.3 Intellectual Property

Shortly after Ames Laboratory successfully converted boron filaments supplied to them by SMI into MgB₂, Ames and SMI began to develop a partnership. Both parties recognized the potential for this technology and agreed that patent protection should be sought quickly. It was agreed that the parties should apply for a joint patent. After filing, and upon advice of legal counsel, it was later agreed that the patent should be segregated into two parts. SMI would be covered for its doping of boron filaments and its boron powder synthesis, while Ames would seek protection for its conversion process to MgB₂. Patent application No. 60/429,137 entitled “Substrate and Method for the Formation of Continuous Magnesium Diboride Wires was filed in the U.S. on Nov. 26, 2002. In addition, a universal foreign patent application (PCT/US03/20628) was filed under the same name on July 1, 2003.

3.0 References

1. J. Nagamatsu, N. Nakagawa, T. Muranaka, Y. Zenitani, and J. Akimitsu, *Nature* **410**, 63 (2001).
2. J.L. MacManus-Driscoll, S.R. Foltyn, Q.X. Jia, H. Wang, A. Serquis, L. Civale, B. Maiorov, M.E. Hawley, M.P. Maley, and D.E. Peterson, *Nature Materials* **3**, 439 (2004).
3. M.P. Parezhantham and T. Izumi, “High-Performance YBCO-Coated Superconductor Wires”, *MRS Bulletin* **29**, 533 (2004); and seven review articles on YBCO-coated conductors that follow in the same issue, pp. 543-589.
4. D.K. Finnemore, W.E. Straszhiem, S.L. Bud’ko, P.C. Canfield, N.E. Anderson Jr., and R.J. Suplinskas, “CVD routes to MgB₂ conductors”, *Physica C*, **385**, 278 (2003).
5. N.E. Anderson Jr., W.E. Straszhiem, S.L. Bud’ko, P.C. Canfield, D.K. Finnemore, and R.J. Suplinskas, “Titanium additions to MgB₂ conductors”, *Physica C*, **390**, 11 (2003).
6. R.H.T. Wilke, S.L. Bud’ko, P.C. Canfield, M.J. Kramer, Y.Q. Wu, D.K. Finnemore, R.J. Suplinskas, J.V. Marzik, S.T. Hannahs, “Superconductivity in MgB₂ doped with Ti and C”, *Physica C* **418**, 160 (2005).
7. R.H.T. Wilke, S.L. Bud’ko, P.C. Canfield, D.K. Finnemore, R.J. Suplinskas, and S.T. Hannahs, “Systematic effects of carbon doping on the superconducting properties of Mg(B_{1-x}C_x)₂”, *Phys. Rev. Lett.* **92**, 217003, 2004.
8. J.V. Marzik, R.J. Suplinskas, R.H.T. Wilke, P.C. Canfield, D.K. Finnemore, M. Rindfleisch, J. Margolies, and S.T. Hannahs, “Plasma synthesized doped B powders for MgB₂ superconductors”, in press, *Physica C*, 2005.
9. X.L. Wang, Q.W. Yao, J. Horvat, M.J. Qin, and S.X. Dou, “Significant improvement of critical current density I coated MgB₂/Cu short tapes through nano-SiC doping and short-time *in situ* reaction”, *Supercond. Sci. Technol.* **17**, L21 (2004).

10. J. Wang, Y. Bugoslavsky, A. Ferenov, L. Cowey, A. D. Caplin, L. F. Cohen, J. L. Driscoll, L. D. Cooley, X. Song, D. C. Larbalestier, *Appl. Phys. Lett.* **81**, 2026 (2002).
11. Y. Zhao, Y. Feng, C.H. Cheng, L. Zhou, Y. Wu, T. Machi, Y. Fudamoto, N. Koshizuka, and M. Murakami, *Appl. Phys. Lett.* **79**, 1154 (2001); Y. Zhao, D.X. Huang, Y. Feng, C.H. Cheng, T. Machi, N. Koshizuka, and M. Murakami, *Appl. Phys. Lett.* **80**, 1640 (2002).
12. S. X. Dou, S. Soltanian, J. Horvat, X. L. Wang, S. H. Zhou, M. Ionescu, H. K. Liu, P. Munroe, and M. Tomsic, "Enhancement of the critical current density and flux pinning of MgB₂ superconductor by nanoparticle SiC doping", *Appl. Phys. Lett.* **81**, 3419 (2002).
13. John D. DeFouw and David C. Dunand, *Appl. Phys. Lett.* **83**, 120 (2003).
14. P.C. Canfield, D.K. Finnemore, S.L. Bud'ko, J.E. Ostenson, G. Lapertot, C.E. Cunningham, and C. Petrovic, *Phys. Rev. Lett.* **86**, 2423, (2001).
15. Raymond J. Suplinskas and James V. Marzik, "Boron and Silicon Carbide Filaments", in *Handbook of Reinforcements for Plastics*, J.V. Milewski and H.S. Katz, editors, (New York: Van Nostrand Reinhold Co.) Ch. 19, 340-363 (1987).
16. P.C. Canfield and G.W. Crabtree, *Physics Today* **56**(3), 34 (2003).
17. P.C. Canfield and S.L. Bud'ko, "Magnesium Diboride: One Year On", *Physics World*, January, 2002
18. P.C. Canfield and S.L. Bud'ko, "Low-Temperature Superconductivity is Warming Up", *Scientific American* **292**, 80-87 (2005).
19. Dunand, D.C., "Synthesis of Superconducting Mg/MgB₂ Composites", *Appl. Phys. Lett.*, 2001. **79**, 4186 (2001).
20. Dunand, D.C., "Superconducting Mg- MgB₂ and Related Metal Composites and Methods of Preparation", US Patent 6,630,427 (2003).
21. Blucher, J.T., U. Narusawa, M. Katsumata, and A. Nemeth, "Continuous manufacturing of fiber-reinforced metal matrix composite wires - technology and product characteristics", *Composites*, **32**, 1759, (2001).
22. Song, X., S.E. Babcock, C.B. Eom, D.C. Larbalestier, K.A. Regan, R.J. Cava, S.L. Bud'Ko, P.C. Canfield, and D.K. Finnemore, "Anisotropic grain morphology, crystallographic texture and their implications for flux pinning mechanisms in MgB₂ pellets, filaments and thin films", *Supercond. Sci. Technol.* **15**, 511 (2002).
23. Zhao, Y., Y. Feng, D.X. Huang, T. Machi, C.H. Cheng, K. Nakao, N. Chikumoto, Y. Fudamoto, N. Koshizuka, and M. Murakami, "Doping effect of Zr and Ti on the critical current density of MgB₂ bulk superconductors prepared under ambient pressure", *Physica C*. **381**, 122 (2002).
24. S. Hamblyn, B. Reuben, and R. Thompson, "Hydrogen reduction of boron trichloride to boron in an R.F. Plasma", *Special Ceramics* **5**, 147 (1970).
25. H.L. Suo, C. Beneduce, X.D. Su, and R. Flukiger, "Fabrication and transport critical currents of multifilamentary MgB₂/Fe wires and tapes", *Supercond. Sci. Technol.* **15**, 1058 (2002).
26. H. Yamada, M. Hirakawa, H. Kumakura, A. Matsumoto, and H. Kitaguchi, "Critical current densities of powder-in-tube MgB₂ tapes fabricated with nanometer-size Mg powder", *Appl. Phys. Lett.* **84**, 1728 (2004).
27. M. Tomsic, Workshop on High Field Intermetallic Superconductors, Montreal, Canada, 24 March 2004.
28. S. Jin, H. Mavoori, C. Bower, and R.B. Van Dover, "High critical currents in iron-clad superconducting MgB₂ wires" *Nature* **411**, 563 (2001).

29. H. Fang, S. Padmanabhan, Y. X. Zhou, and K. Salama, "High critical current density in iron-clad MgB₂ tapes", *Appl. Phys. Lett.* **82**, 4113 (2003).
30. H.L. Suo, C. Beneduce, M. Dhallé, N. Musolino, J-Y. Genoud, and R. Flükiger, "Large transport critical currents in dense Fe- and Ni-clad MgB₂ superconducting tapes," *Appl. Phys. Lett.* **79**, 3116 (2001).
31. A.C. Serquis, L. Civale, X. Liao, D.L. Hammon, J.Y. Coulter, V.F. Nesterenko, Y.T. Zhu, F.M. Mueller, and D.E. Peterson, "Processing and Characterization of Powder in Tube MgB₂ wires", *Frontiers in Superconducting Materials – New Materials and Applications*, Materials Research Society Symposium Proceedings Series, Warrendale, PA: Materials Research Society, in press, 2004.
32. Maciszewski and W. Scharf, "Particle Accelerators for Radiotherapy: Present Status and Future", Proceedings of the 8th International Conference on Advanced Technology and Particle Physics, Como, Italy (2003).
33. L.D. Cooley, A.K. Ghosh, and R.M. Scanlan, "Costs of High-Field Superconducting Strands for Particle Accelerator Magnets", *Supercond. Sci. and Technol.* **18**, R51 (2005).
34. J. DeFouw, D. Dunand, J. Marzik, R. Suplinskas, J. Quintana, "Processing, Microstructure, and Properties of Doped and Undoped MgB₂ Fibers", presented at the March Meeting of the American Physical Society, Los Angeles, CA, March, 2005.
35. J.V. Marzik, R.J. Suplinskas, W.J. Croft, W.J. MoberlyChan, J.D. DeFouw, and D.C. Dunand, "The effect of dopant additions on the microstructure of boron fibers before and after reaction to MgB₂", In press, Symposium FF Proceedings, Fall 2004 Materials Research Society Conference (2005).
36. J.L. Hoard, R.E. Hughes, D.E. Sands, *J. Am. Chem. Soc.* **80**, 4507 (1958).
37. International Center for Diffraction Data: Newtown Square, PA (2004).
38. ASM Handbook, Volume 3, Alloy Phase Diagrams, (1992).